# Structured Catalysts and Reactors

## Second Edition

## CHEMICAL INDUSTRIES

A Series of Reference Books and Textbooks

*Series Editor*

**JAMES G. SPEIGHT**
*Laramie, Wyoming*

*Founding Editor*

**HEINZ HEINEMANN**
*Berkeley, California*

1. *Fluid Catalytic Cracking with Zeolite Catalysts,* Paul B. Venuto and E. Thomas Habib, Jr.
2. *Ethylene: Keystone to the Petrochemical Industry,* Ludwig Kniel, Olaf Winter, and Karl Stork
3. *The Chemistry and Technology of Petroleum,* James G. Speight
4. *The Desulfurization of Heavy Oils and Residua,* James G. Speight
5. *Catalysis of Organic Reactions,* edited by William R. Moser
6. *Acetylene-Based Chemicals from Coal and Other Natural Resources,* Robert J. Tedeschi
7. *Chemically Resistant Masonry,* Walter Lee Sheppard, Jr.
8. *Compressors and Expanders: Selection and Application for the Process Industry,* Heinz P. Bloch, Joseph A. Cameron, Frank M. Danowski, Jr., Ralph James, Jr., Judson S. Swearingen, and Marilyn E. Weightman
9. *Metering Pumps: Selection and Application,* James P. Poynton
10. *Hydrocarbons from Methanol,* Clarence D. Chang
11. *Form Flotation: Theory and Applications,* Ann N. Clarke and David J. Wilson
12. *The Chemistry and Technology of Coal,* James G. Speight
13. *Pneumatic and Hydraulic Conveying of Solids,* O. A. Williams
14. *Catalyst Manufacture: Laboratory and Commercial Preparations,* Alvin B. Stiles
15. *Characterization of Heterogeneous Catalysts,* edited by Francis Delannay
16. *BASIC Programs for Chemical Engineering Design,* James H. Weber
17. *Catalyst Poisoning,* L. Louis Hegedus and Robert W. McCabe
18. *Catalysis of Organic Reactions,* edited by John R. Kosak
19. *Adsorption Technology: A Step-by-Step Approach to Process Evaluation and Application,* edited by Frank L. Slejko
20. *Deactivation and Poisoning of Catalysts,* edited by Jacques Oudar and Henry Wise

21. *Catalysis and Surface Science: Developments in Chemicals from Methanol, Hydrotreating of Hydrocarbons, Catalyst Preparation, Monomers and Polymers, Photocatalysis and Photovoltaics,* edited by Heinz Heinemann and Gabor A. Somorjai
22. *Catalysis of Organic Reactions,* edited by Robert L. Augustine
23. *Modern Control Techniques for the Processing Industries,* T. H. Tsai, J. W. Lane, and C. S. Lin
24. *Temperature-Programmed Reduction for Solid Materials Characterization,* Alan Jones and Brian McNichol
25. *Catalytic Cracking: Catalysts, Chemistry, and Kinetics,* Bohdan W. Wojciechowski and Avelino Corma
26. *Chemical Reaction and Reactor Engineering,* edited by J. J. Carberry and A. Varma
27. *Filtration: Principles and Practices: Second Edition,* edited by Michael J. Matteson and Clyde Orr
28. *Corrosion Mechanisms,* edited by Florian Mansfeld
29. *Catalysis and Surface Properties of Liquid Metals and Alloys,* Yoshisada Ogino
30. *Catalyst Deactivation,* edited by Eugene E. Petersen and Alexis T. Bell
31. *Hydrogen Effects in Catalysis: Fundamentals and Practical Applications,* edited by Zoltán Paál and P. G. Menon
32. *Flow Management for Engineers and Scientists,* Nicholas P. Cheremisinoff and Paul N. Cheremisinoff
33. *Catalysis of Organic Reactions,* edited by Paul N. Rylander, Harold Greenfield, and Robert L. Augustine
34. *Powder and Bulk Solids Handling Processes: Instrumentation and Control,* Koichi Iinoya, Hiroaki Masuda, and Kinnosuke Watanabe
35. *Reverse Osmosis Technology: Applications for High-Purity-Water Production,* edited by Bipin S. Parekh
36. *Shape Selective Catalysis in Industrial Applications,* N. Y. Chen, William E. Garwood, and Frank G. Dwyer
37. *Alpha Olefins Applications Handbook,* edited by George R. Lappin and Joseph L. Sauer
38. *Process Modeling and Control in Chemical Industries,* edited by Kaddour Najim
39. *Clathrate Hydrates of Natural Gases,* E. Dendy Sloan, Jr.
40. *Catalysis of Organic Reactions,* edited by Dale W. Blackburn
41. *Fuel Science and Technology Handbook,* edited by James G. Speight
42. *Octane-Enhancing Zeolitic FCC Catalysts,* Julius Scherzer
43. Oxygen in Catalysis, Adam Bielanski and Jerzy Haber
44. *The Chemistry and Technology of Petroleum: Second Edition, Revised and Expanded,* James G. Speight
45. *Industrial Drying Equipment: Selection and Application,* C. M. van't Land
46. *Novel Production Methods for Ethylene, Light Hydrocarbons, and Aromatics*, edited by Lyle F. Albright, Billy L. Crynes, and Siegfried Nowak
47. *Catalysis of Organic Reactions*, edited by William E. Pascoe
48. *Synthetic Lubricants and High-Performance Functional Fluids*, edited by Ronald L. Shubkin
49. *Acetic Acid and Its Derivatives*, edited by Victor H. Agreda and Joseph R. Zoeller
50. *Properties and Applications of Perovskite-Type Oxides*, edited by L. G. Tejuca and J. L. G. Fierro
51. *Computer-Aided Design of Catalysts*, edited by E. Robert Becker and Carmo J. Pereira

52. *Models for Thermodynamic and Phase Equilibria Calculations*, edited by Stanley I. Sandler
53. *Catalysis of Organic Reactions*, edited by John R. Kosak and Thomas A. Johnson
54. *Composition and Analysis of Heavy Petroleum Fractions*, Klaus H. Altgelt and Mieczyslaw M. Boduszynski
55. *NMR Techniques in Catalysis,* edited by Alexis T. Bell and Alexander Pines
56. *Upgrading Petroleum Residues and Heavy Oils*, Murray R. Gray
57. *Methanol Production and Use*, edited by Wu-Hsun Cheng and Harold H. Kung
58. *Catalytic Hydroprocessing of Petroleum and Distillates*, edited by Michael C. Oballah and Stuart S. Shih
59. *The Chemistry and Technology of Coal: Second Edition, Revised and Expanded,* James G. Speight
60. *Lubricant Base Oil and Wax Processing*, Avilino Sequeira, Jr.
61. *Catalytic Naphtha Reforming: Science and Technology*, edited by George J. Antos, Abdullah M. Aitani, and José M. Parera
62. *Catalysis of Organic Reactions*, edited by Mike G. Scaros and Michael L. Prunier
63. *Catalyst Manufacture,* Alvin B. Stiles and Theodore A. Koch
64. *Handbook of Grignard Reagents,* edited by Gary S. Silverman and Philip E. Rakita
65. *Shape Selective Catalysis in Industrial Applications: Second Edition, Revised and Expanded*, N. Y. Chen, William E. Garwood, and Francis G. Dwyer
66. *Hydrocracking Science and Technology*, Julius Scherzer and A. J. Gruia
67. *Hydrotreating Technology for Pollution Control: Catalysts, Catalysis, and Processes*, edited by Mario L. Occelli and Russell Chianelli
68. *Catalysis of Organic Reactions*, edited by Russell E. Malz, Jr.
69. *Synthesis of Porous Materials: Zeolites, Clays, and Nanostructures,* edited by Mario L. Occelli and Henri Kessler
70. *Methane and Its Derivatives*, Sunggyu Lee
71. *Structured Catalysts and Reactors*, edited by Andrzej Cybulski and Jacob A. Moulijn
72. *Industrial Gases in Petrochemical Processing*, Harold Gunardson
73. *Clathrate Hydrates of Natural Gases: Second Edition, Revised and Expanded*, E. Dendy Sloan, Jr.
74. *Fluid Cracking Catalysts*, edited by Mario L. Occelli and Paul O'Connor
75. *Catalysis of Organic Reactions*, edited by Frank E. Herkes
76. *The Chemistry and Technology of Petroleum: Third Edition, Revised and Expanded*, James G. Speight
77. *Synthetic Lubricants and High-Performance Functional Fluids: Second Edition, Revised and Expanded,* Leslie R. Rudnick and Ronald L. Shubkin
78. *The Desulfurization of Heavy Oils and Residua*, *Second Edition*, *Revised and Expanded,* James G. Speight
79. *Reaction Kinetics and Reactor Design: Second Edition, Revised and Expanded,* John B. Butt
80. *Regulatory Chemicals Handbook*, Jennifer M. Spero, Bella Devito, and Louis Theodore
81. *Applied Parameter Estimation for Chemical Engineers*, Peter Englezos and Nicolas Kalogerakis
82. *Catalysis of Organic Reactions,* edited by Michael E. Ford
83. *The Chemical Process Industries Infrastructure: Function and Economics*, James R. Couper, O. Thomas Beasley, and W. Roy Penney
84. *Transport Phenomena Fundamentals*, Joel L. Plawsky

85. *Petroleum Refining Processes*, James G. Speight and Baki Özüm
86. *Health, Safety, and Accident Management in the Chemical Process Industries*, Ann Marie Flynn and Louis Theodore
87. *Plantwide Dynamic Simulators in Chemical Processing and Control*, William L. Luyben
88. *Chemicial Reactor Design*, Peter Harriott
89. *Catalysis of Organic Reactions*, edited by Dennis G. Morrell
90. *Lubricant Additives: Chemistry and Applications*, edited by Leslie R. Rudnick
91. *Handbook of Fluidization and Fluid-Particle Systems*, edited by Wen-Ching Yang
92. *Conservation Equations and Modeling of Chemical and Biochemical Processes*, Said S. E. H. Elnashaie and Parag Garhyan
93. *Batch Fermentation: Modeling, Monitoring, and Control*, Ali Çinar, Gülnur Birol, Satish J. Parulekar, and Cenk Ündey
94. *Industrial Solvents Handbook, Second Edition*, Nicholas P. Cheremisinoff
95. *Petroleum and Gas Field Processing*, H. K. Abdel-Aal, Mohamed Aggour, and M. Fahim
96. *Chemical Process Engineering: Design and Economics*, Harry Silla
97. *Process Engineering Economics*, James R. Couper
98. *Re-Engineering the Chemical Processing Plant: Process Intensification*, edited by Andrzej Stankiewicz and Jacob A. Moulijn
99. *Thermodynamic Cycles: Computer-Aided Design and Optimization*, Chih Wu
100. *Catalytic Naptha Reforming: Second Edition, Revised and Expanded*, edited by George T. Antos and Abdullah M. Aitani
101. *Handbook of MTBE and Other Gasoline Oxygenates*, edited by S. Halim Hamid and Mohammad Ashraf Ali
102. *Industrial Chemical Cresols and Downstream Derivatives*, Asim Kumar Mukhopadhyay
103. *Polymer Processing Instabilities: Control and Understanding*, edited by Savvas Hatzikiriakos and Kalman B . Migler
104. *Catalysis of Organic Reactions*, John Sowa
105. *Gasification Technologies: A Primer for Engineers and Scientists*, edited by John Rezaiyan and Nicholas P. Cheremisinoff
106. *Batch Processes*, edited by Ekaterini Korovessi and Andreas A. Linninger
107. *Introduction to Process Control*, Jose A. Romagnoli and Ahmet Palazoglu
108. *Metal Oxides: Chemistry and Applications*, edited by J. L. G. Fierro
109. *Molecular Modeling in Heavy Hydrocarbon Conversions*, Michael T. Klein, Ralph J. Bertolacini, Linda J. Broadbelt, Ankush Kumar and Gang Hou
110. *Structured Catalysts and Reactors, Second Edition*, edited by Andrzej Cybulski and Jacob A. Moulijn

# Structured Catalysts and Reactors

## Second Edition

edited by
Andrzej Cybulski
Jacob A. Moulijn


Taylor & Francis
Taylor & Francis Group
Boca Raton London New York

A CRC title, part of the Taylor & Francis imprint, a member of the Taylor & Francis Group, the academic division of T&F Informa plc.

Published in 2006 by
CRC Press
Taylor & Francis Group
6000 Broken Sound Parkway NW, Suite 300
Boca Raton, FL 33487-2742


Printed in the United States of America on acid-free paper
10 9 8 7 6 5 4 3 2 1

International Standard Book Number-10: 0-8247-2343-0 (Hardcover)
International Standard Book Number-13: 978-0-8247-2343-9 (Hardcover)
Library of Congress Card Number 2005049124



**Library of Congress Cataloging-in-Publication Data**

Structured catalysts and reactors / [edited by] Andrzej Cybulski and Jacob A. Moulijn.--2nd ed.
p. cm. -- (Chemical industries series ; v. 110)
Includes bibliographical references.
ISBN 0-8247-2343-0 (acid-free paper)
1. Catalysts. 2. Chemical reactors. I. Cybulski, Andrzej, 1938- II. Moulijn, Jacob A. III. Chemical industries ; v. 110.

TP156.C35S77 2005
660'.2995--dc22 2005049124

informa
Taylor & Francis Group
is the Academic Division of Informa plc.

**Visit the Taylor & Francis Web site at**
**http://www.taylorandfrancis.com**

**and the CRC Press Web site at**
**http://www.crcpress.com**

# Preface

Heterogeneous catalytic processes are among the main ways to decrease the consumption of raw materials in chemical industries and to decrease the emission of pollutants of all kinds to the environment via an increase in process selectivity. Selectivity can be improved by the modification of catalyst composition and surface structure and/or by the modification of pellet dimensions, shape, and texture, i.e., pore size distribution, pore shape, length, and cross-sectional surface area (distribution). Until recently, the limiting factor in the latter modifications has been the particles' size, to which the length of diffusion in pores is related. The size should not be too small because of the significantly higher pressure drop for such small particles. Shell catalysts, which contain catalytic species concentrated near the outer particles' surface, are a remedy for improving selectivity and keeping pressure drop at a reasonable level. Pressure drop can be the limiting factor even for such catalysts, e.g., when large quantities of raw materials must be processed or when the higher pressure drop results in a significantly higher consumption of raw materials. For instance, converting huge amounts of natural gas in remote areas would require equipment characterized by low pressure drop. Otherwise the cost of processing would be too high to make the process economical. Too high a pressure drop in catalytic car mufflers would result in an increase in fuel consumption by several percent. This would mean a several-percent-higher consumption of crude oil for transportation. An inherent feature of conventional packed-bed reactors is their random and structural maldistributions. A structural maldistribution in fixed-bed reactors originates from the looser packing of particles near the reactor walls. This results in a tendency to bypass the core of the bed, even if the initial distribution of fluid(s) is uniform. The uniformly distributed liquid tends to flow to the walls, and this can drastically alter its residence time from the design value. Random maldistributions result in: (1) a nonuniform access of reactants to the catalytic surface, worsening the overall process performance, and (2) unexpected hot spots and thermal runaways of exothermic reactions (mainly in three-phase reactions).

Structured catalysts (reactors) are promising as far as the elimination of these drawbacks of fixed beds is concerned. Three basic kinds of structured catalysts can be distinguished:

1. *Monolithic catalysts (honeycomb catalysts)*, in the form of continuous unitary structures that contain small passages. The catalytically active material is present on or inside the walls of these passages. In the former case, a ceramic or metallic support is coated with a layer of material in which active ingredients are dispersed.
2. *Membrane catalysts* are structures with permeable walls between passages. The membrane walls exhibit selectivity in transport rates for the various components present. A slow radial mass transport can occur, driven by diffusion or solution/diffusion mechanisms in the permeable walls.
3. *Arranged catalysts*. Particulate catalysts arranged in *arrays* belong to this class of structured catalysts. Another group of arranged catalysts are *structural catalysts*, derived from structural packings for distillation and absorption columns and static mixers. These are structures consisting of superimposed sheets, possibly corrugated before stacking. The sheets are covered by an appropriate catalyst support in which active ingredients are incorporated. The structure is an open cross-flow structure characterized by intensive radial mixing.

Usually, structured catalysts are structures of large void fraction ranging from 0.7 to more than 0.9, compared to 0.5 in packed beds. The path the fluids follow in structured reactors is much less twisted (e.g., straight channels in monoliths) than that in conventional reactors. Finally, structured reactors are operated in a different hydrodynamic regime. For single-phase flow the regime is laminar, and the eddies characteristic of packed beds are absent. For multiphase systems various regimes exist, but here also eddies are absent. For these reasons, the pressure drop in structured catalysts is significantly lower than that in randomly packed beds of particles. Indeed, the pressure drop in monolithic reactors is up to two orders of magnitude lower than that in packed-bed reactors.

Catalytic species are incorporated either into a very thin layer of a porous catalyst support deposited on the structured elements or into the thin elements themselves. The short diffusion distance inside the thin layer of the structured catalysts results in higher catalyst utilization and can contribute to an improvement of selectivity for processes controlled by mass transfer within the catalytic layer. In contrast to conventional packed-bed reactors, the thickness of the catalytic layer in monolithic reactors can be significantly reduced with no penalty paid for the increase in pressure drop. Membrane catalysts provide a unique opportunity to supply reactants to the reaction mixture gradually along the reaction route or to withdraw products from the reaction mixture as they are formed. The former mode of carrying out complex reactions might be very effective in controlling undesired reactions whose rates are strongly dependent on the concentration of the added reactant. The latter mode might result in higher conversions for reversible reactions, which are damped by products. The use of catalytic membranes operated in any of these modes can also contribute to significant improvement in selectivity. The regular structure of the arranged catalysts prevents the formation of the random maldistributions characteristic of beds of randomly packed particles. This reduces the probability of the occurrence of hot spots resulting from flow maldistributions.

Scale-up of monolithic and membrane reactors can be expected to be straightforward, since the conditions within the individual channels are scale invariant.

Finally, structured catalysts and reactors constitute a significant contribution to the search for better catalytic processes via improving mass transfer in the catalytic layer and thus improving activity and selectivity, decreasing operating costs through lowering the pressure drop, and eliminating maldistributions.

Structured catalysts, mainly monolithic ones, are now used predominantly in environmental applications, first of all in the cleaning of automotive exhaust gases. Monolithic reactors have become the most commonly used sort of chemical reactors: nearly a billion small monolithic reactors are moving with our cars! Monolithic cleaners of flue gases are now standard units. Monolithic catalysts are also close to commercialization in the combustion of fuels for gas turbines, boilers, heaters, etc. The catalytic combustion reduces $NO_x$ formation, and the use of low-pressure-drop catalysts makes the process more economical. Some special features of monolithic catalysts make the burning of low-heating-value (LHV) fuels in monolithic units much easier than in packed beds of particulate catalysts. There are some characteristics that make structured catalysts also of interest for three-phase reactions. Several three-phase processes are in the development stage. Catalytic oxidation of organics in wastewater is currently operated in demonstration plants. One process, the hydrogenation step in the production of hydrogen peroxide using the alkylanthraquinone process, has already reached full scale, with several plants in operation.

Interest in structured catalysts is steadily increasing due to the already proven, and potential, advantages of these catalysts. A number of review articles regarding different aspects of structured catalysts have been published in the last decade [see F. Kapteijn, J.J. Heiszwolf, T.A. Nijhuis, and J.A. Moulijn, *Cattech*, 3, 24–41, 1999; A. Cybulski and J.A. Moulijn, *Catal. Rev. Sci. Eng*., 36, 179–270, 1994; G. Saracco and V. Specchia, *Catal.*

*Rev. Sci. Eng.*, 36, 305–384, 1994; H.P. Hsieh, *Catal. Rev. Sci. Eng.*, 33, 1–70, 1991; S. Irandoust and B. Anderson, *Catal. Rev. Sci. Eng.*, 30, 341–392, 1988; and L.D. Pfefferle and W.C. Pfefferle, *Catal. Rev. Sci. Eng.*, 29, 219–267, 1987].

These articles do not cover the whole area of structured catalysts and reactors. Moreover, the science and applications of structured catalysts and reactors are developing very fast. Therefore, some eight years ago we decided to edit a book on structured catalysts and reactors. In 1998 it was published. The time has now come for an updated version. In this edition an attempt has been made to give detailed information on all structures known to date and on all aspects of structured catalysts and reactors containing them: catalyst preparation and characterization, catalysts and process development, modeling and optimization, and finally reactor design and operation. As such, the book is dedicated to all readers who are involved in the development of catalytic processes, from R&D to process engineering. A very important area of structuring in catalysis is that directed at a catalytic surface, microstructure, and structuring the shape and size of the catalytic bodies. This area is essentially covered by publications concerning a more fundamental approach to heterogeneous catalysis. A lot of the relevant information is scale dependent and, as a consequence, is not unique to structured catalytic reactors. Therefore, these activities are described only briefly in this book.

The book starts with an overview on structured catalysts (Chapter 1). The rest of the book is divided in four parts. The first three parts deal with structures differing from each other significantly in conditions for mass transfer in the reaction zone. The fourth part is dedicated to catalyst design and preparation.

Part I deals with monolithic catalysts. Chapters 2 and 3 deal with the configurations, microstructure, physical properties, and manufacture of ceramic and metallic monoliths. Monolithic catalysts for cleaning the exhaust gas from gasoline-fueled engines are dealt with in Chapter 4, including fundamentals and exploitation experience. Chapters 5 and 6 are devoted to commercial and developmental catalysts for protecting the environment. The subject of Chapter 5 is the treatment of volatile organic carbon (VOC) emissions from stationary sources. In Chapter 6 fundamentals and applications of monoliths for selective catalytic reduction of $NO_x$ are given. Unconventional reactors used in this field (reverse-flow reactors, rotating monoliths) are also discussed. Materials, activity, and stability of catalysts for catalytic combustion and practical applications of monolithic catalysts in this area are discussed in Chapter 7. The use of monolithic catalysts for the synthesis of chemicals is discussed in Chapter 8. Chapter 9 is devoted to the modeling of monolithic catalysts for two-phase processes (gaseous reactants/solid catalyst). Chapters 10–13 deal with three-phase monolithic processes. Both catalytic and engineering aspects of these processes are discussed.

Arranged catalysts allowing for convective mass transfer over the cross section of the reactor are discussed in Part II. Conventional particulate catalysts arranged in arrays are dealt with in Chapter 14. Current and potential applications of ordered structures of different kinds (parallel-passage and lateral-flow reactors) are mentioned. Chapter 15 is devoted to structured packings with respect to reactive distillation with emphasis on Sulzer Katapak-SP packings.

Part III of the book provides information about structured catalysts of the monolithic type with permeable walls, i.e., catalytically active membranes. Chapter 16 deals with catalytic filters for flue gas cleaning.

Catalytic membranes create a unique opportunity to couple processes opposite in character (e.g., hydrogenation/dehydrogenation, endothermic/exothermic) via the combination of reaction and separation. Catalytic membranes can allow for the easy control of reactant addition or product withdrawal along the reaction route. Chapter 17 deals with membrane reactors with metallic walls permeable to some gases. The properties of metallic membranes, permeation mechanisms in metallic membranes, the preparation of membranes,

commercial membranes, modeling and design, engineering and operating considerations, and finally current and potential applications of metallic membranes are discussed. Chapter 18 presents inorganic membrane reactors: materials, membrane microstructures, commercial membranes, modeling and design, engineering and operating issues, and current and potential applications. Chapter 19 is dedicated to a special type of catalytic filters used for cleaning exhausts from diesel engines. Recent developments in the field of advanced membranes, in the form of zeolitic membranes are discussed in Chapter 20.

The last part of the book (Part IV) discusses techniques for incorporating catalytic species into the structured catalyst support (Chapter 21) and structuring of catalyst nanoporosity (Chapter 22).

The amount of detail in this book varies, depending on whether the catalyst/reactor is in the developmental stage or already has been commercialized. The know-how gained in process development has commercial value, and this usually inhibits the presentation of the details of the process/reactor/catalyst. Consequently, well-established processes/reactors/catalysts are described more generally. Projects at an earlier stage presented in this book are being developed at universities, which usually reveal more details. Each chapter was designed as a whole that can be read without reference to the others. Therefore, repetitions and overlapping (and sometimes also contradictions) between the chapters of this book are unavoidable.

The authors of individual chapters are top specialists in their areas. They comprise an international group of scientists and practitioners (Great Britain, Italy, The Netherlands, Poland, Russia, Sweden, Switzerland, and the U.S.) from universities and companies that are advanced in the technology of structured catalysts. The editors express their gratitude to all of the contributors for sharing their experience. The editors also appreciate the great help of Annelies van Diepen in shaping the book and its chapters.

# Contributors

**Rolf Edvinsson Albers**
R & D Pulp & Paper
Eka Chemicals
Bohus, Sweden

**Bengt Andersson**
Department of Chemical Reaction Engineering
Chalmers University of Technology
Göteborg, Sweden

**Oliver Bailer**
Sulzer Chemtech Ltd
Winterthur, Switzerland

**Alessandra Beretta**
Dipartimento di Chimica, Materiali e Ingegneria Chimica "Giulio Natta"
Politecnico di Milano
Milano, Italy

**Hans Peter Calis**
Delft University of Technology
Delft, The Netherlands

**Marc-Olivier Coppens**
Delft University of Technology
DelftChemTech
Delft, The Netherlands

**Andrzej Cybulski**
Polish Academy of Sciences
CHEMIPAN, Institute of Physical Chemistry
Warsaw, Poland

**Margarita M. Ermilova**
Topchiev Institute of Petrochemical Synthesis
Russian Academy of Sciences
Moscow, Russia

**Anders G. Ersson**
KTH – Royal Institute of Technology
Stockholm, Sweden

**Debora Fino**
Dipartimento di Scienza dei Materiali ed Ingegneria Chimica
Politecnico di Torino
Torino, Italy

**Pio Forzatti**
Dipartimento di Chimica, Materiali e Ingegneria Chimica "Giulio Natta"
Politecnico di Milano
Milano, Italy

**Tracy Q. Gardner**
Chemical Engineering Department
Colorado School of Mines
Golden, Colorado

**Gianpiero Groppi**
Dipartimento di Chimica, Materiali e Ingegneria Chimica "Giulio Natta"
Politecnico di Milano
Milano, Italy

**Vladimir M. Gryaznov (deceased)**
Topchiev Institute of Petrochemical Synthesis
Russian Academy of Sciences
Moscow, Russia

**Suresh T. Gulati**
Corning Incorporated
Science & Technology Division
Corning, New York

**Jan M.A. Harmsen**
Ford Forschungszentrum Aachen
Aachen, Germany

**Achim K. Heibel**
Corning Incorporated
Corning Environmental Technologies
Corning, New York

**Jozef H.B.J. Hoebink**
Laboratory of Chemical Reactor Engineering
Eindhoven University of Technology
Eindhoven, The Netherlands

**Sven G. Järås**
KTH – Royal Institute of Technology
Stockholm, Sweden

**Freek Kapteijn**
Delft University of Technology
Reactor and Catalysis Engineering
Delft, The Netherlands

**Stan Kolaczkowski**
Department of Chemical Engineering
University of Bath
Bath, U.K.

**Michiel T. Kreutzer**
Reactor and Catalysis Engineering
Delft University of Technology
Delft, The Netherlands

**Paul J.M. Lebens**
Albemarle Catalysts
Amsterdam, The Netherlands

**Luca Lietti**
Dipartimento di Chimica, Materiali e Ingegneria Chimica "Giulio Natta"
Politecnico di Milano
Milano, Italy

**Michiel Makkee**
Reactor and Catalysis Engineering
Delft University of Technology
Delft, The Netherlands

**Guy B. Marin**
Laboratorium voor Petrochemische Techniek
Universiteit Gent
Gent, Belgium

**Jacob A. Moulijn**
Reactor and Catalysis Engineering
Delft University of Technology
Delft, The Netherlands

**Isabella Nova**
Dipartimento di Chimica, Materiali e Ingegneria Chimica "Giulio Natta"
Politecnico di Milano
Milano, Italy

**Natalia V. Orekhova**
Topchiev Institute of Petrochemical Synthesis
Russian Academy of Sciences
Moscow, Russia

**Guido Saracco**
Dipartimento di Scienza dei Materiali ed Ingegneria Chimica
Politecnico di Torino
Torino, Italy

**Claudia von Scala**
Sulzer Chemtech Ltd
Winterthur, Switzerland

**Caren M.L. Scholz**
Laboratory of Chemical Reactor Engineering
Eindhoven University of Technology
Eindhoven, The Netherlands

**Jaap C. Schouten**
Laboratory of Chemical Reactor Engineering
Eindhoven University of Technology
Eindhoven, The Netherlands

**Agus Setiabudi**
Reactor and Catalysis Engineering
Delft University of Technology
Delft, The Netherlands

**Swan Tiong Sie**
Delft University of Technology
Delft, The Netherlands

**Stefania Specchia**
Dipartimento di Scienza dei Materiali ed Ingegneria Chimica
Politecnico di Torino
Torino, Italy

**Vito Specchia**
Dipartimento di Scienza dei Materiali ed Ingegneria Chimica
Politecnico di Torino
Torino, Italy

**Lothar Spiegel**
Sulzer Chemtech Ltd
Winterthur, Switzerland

**Gennady F. Tereschenko**
Topchiev Institute of Petrochemical Synthesis
Russian Academy of Sciences
Moscow, Russia

**Enrico Tronconi**
Dipartimento di Chimica, Materiali e Ingegneria Chimica "Giulio Natta"
Politecnico di Milano
Milano, Italy

**Martyn V. Twigg**
Johnson Matthey Catalysts
Environmental Catalysts and Technologies
Royston, U.K.

**Dennis E. Webster**
Johnson Matthey Catalysts
Environmental Catalysts and Technologies
Royston, U.K.

**Anthony J.J. Wilkins**
Johnson Matthey Catalysts
Environmental Catalysts and Technologies
Royston, U.K.

**Xiaoding Xu**
Reactor and Catalysis Engineering
Delft University of Technology
Delft, The Netherlands

**Weidong Zhu**
Reactor and Catalysis Engineering
Delft University of Technology
Delft, The Netherlands

# Table of Contents

# 19 Ceramic Catalysts, Supports, and Filters for Diesel Exhaust After-Treatment

*Suresh T. Gulati, Michiel Makkee, and Agus Setiabudi*

**CONTENTS**

## 19.1 INTRODUCTION

### 19.1.1 Diesel Soot Formation

Since the invention by Rudolf Diesel in 1893, the application of the diesel engine has become very widespread across the world. The popularity of the diesel engine is a result of its attractive characteristics, such as fuel economy, durability, low maintenance requirements, and large indifference to fuel specification. Fuel efficiency for a diesel engine is 30 to 50% higher than that for a gasoline engine with comparable power. In other words the $CO_2$ emission will be 30 to 50% lower for a diesel engine for the same amount of generated power. $CO_2$ is one of the main greenhouse gases and contributes to global warning. If one wants to reduce the emission of $CO_2$ and at the same time maintain mobility via transportation, a transition from gasoline-powered engines to diesel-powered engines is a logical choice. Diesel engines are used in various fields. Transport applications of the diesel engine can be found in light passenger cars, trucks, construction equipment, and ships. Another large field of application is that of stationary power sources. Many electricity and hydraulic power plants are equipped with diesel engines.

Unfortunately, the reality of most combustion engines, including diesel engines, is that they encounter the problem of incomplete combustion, which leads to the emission of severe diesel pollutants.

During operation diesel fuel is injected into the cylinder. The liquid atomizes into small droplets, which vaporize and mix with air under pressure and burn. Fuel distribution is nonuniform, and the generation of unwanted emissions is highly dependent on the degree of nonuniformity. Carbonaceous soot is formed in the center of the fuel spray where the air/fuel ratio is low. Nonideal mixing of fuel and air creates small pockets of excess fuel where the solid carbonaceous soot particles (a solid and a soluble organic fraction, SOF) are formed [1–3].

Associated with carbonaceous soot, adsorbed hydrocarbons and small amounts of sulfates, nitrates, metals, trace elements, water, and unidentified compounds make up the diesel particulate matter (PM). A transmission electron microscopy (TEM) image and a schematic of the structure and composition of PM are shown in Figure 19.1 and Figure 19.2, respectively. Figure 19.3 illustrates the process of soot formation.

Adsorbed hydrocarbon, sulfate, and water act as "glue," causing multiple particles to agglomerate and shift the particle size and mass distribution upward [5]. PM is typically composed of more than 50% to approximately 75% elemental carbon (EC) depending on the age of the engine, deterioration, heavy duty versus light duty, fuel characteristics, and driving conditions. The hydrocarbon portion of PM originates from unburned fuel, engine lubrication oil, low levels of partial combustion, and pyrolysis products, and typically ranges from approximately 19 to 43%, although the range can be broader depending on many of the same factors that influence the EC content of PM. Polyaromatic hydrocarbons generally constitute less than 1% of the PM mass. Metal compounds and other elements in the fuel and engine lubrication oil are emitted as ash and typically make up 1 to 5% of the PM mass. Elements and metals detected in diesel emissions include barium, calcium, chlorine, chromium, copper, iron, lead, manganese, mercury, nickel, phosphorus, sodium, silicon, and zinc [4,5,8].

Together with particulate emissions, CO, hydrocarbon (HC), and $NO_x$ are emitted as diesel exhaust gaseous pollutants. As with the formation of soot, CO and HC are the results of incomplete combustion. In contrast with soot formation, $NO_x$ is created where the air/fuel ratio approaches stoichiometry and high temperatures are generated [9].

The output range of basic toxic material, the temperature, and the exhaust mass flow rate are summarized in Table 19.1. For gas and PM emissions, the lower values can be

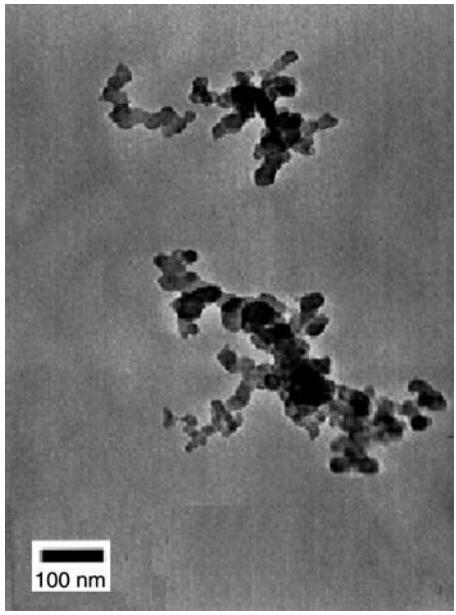


**FIGURE 19.1** TEM image of PM $< 10\,\mu m$ (PM10) collected by impaction for 30 sec. (After Bérubé, K.A., Jones, T.P., Williamson, B.J., Winters, C., Morgan, A.J., and Richards, R.J., *Atmos. Environ.*, 33, 1599–1614, 1999.)

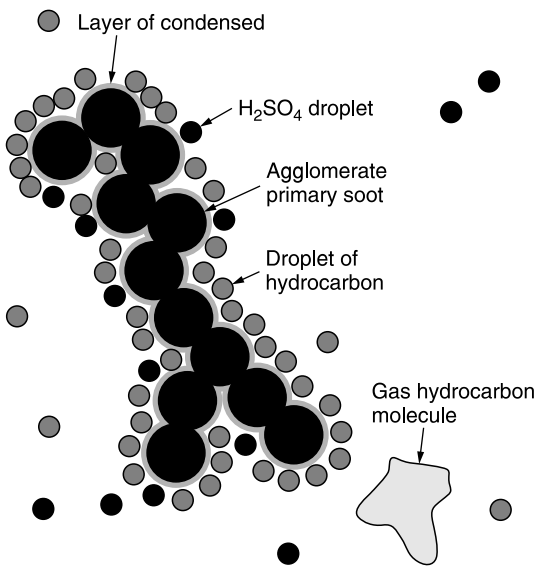


**FIGURE 19.2** Schematic of diesel soot and its adsorbed species. (After Mark, J. and Morey, C., *Diesel Passenger Vehicles and the Environment*, Union of Concerned Scientists, Berkeley, CA, 1999, pp. 6–15 and Johnson, J.H., Bagley, S.T., Gratz, L.D., Leddy, D.G., SAE paper 940233, 1994.)

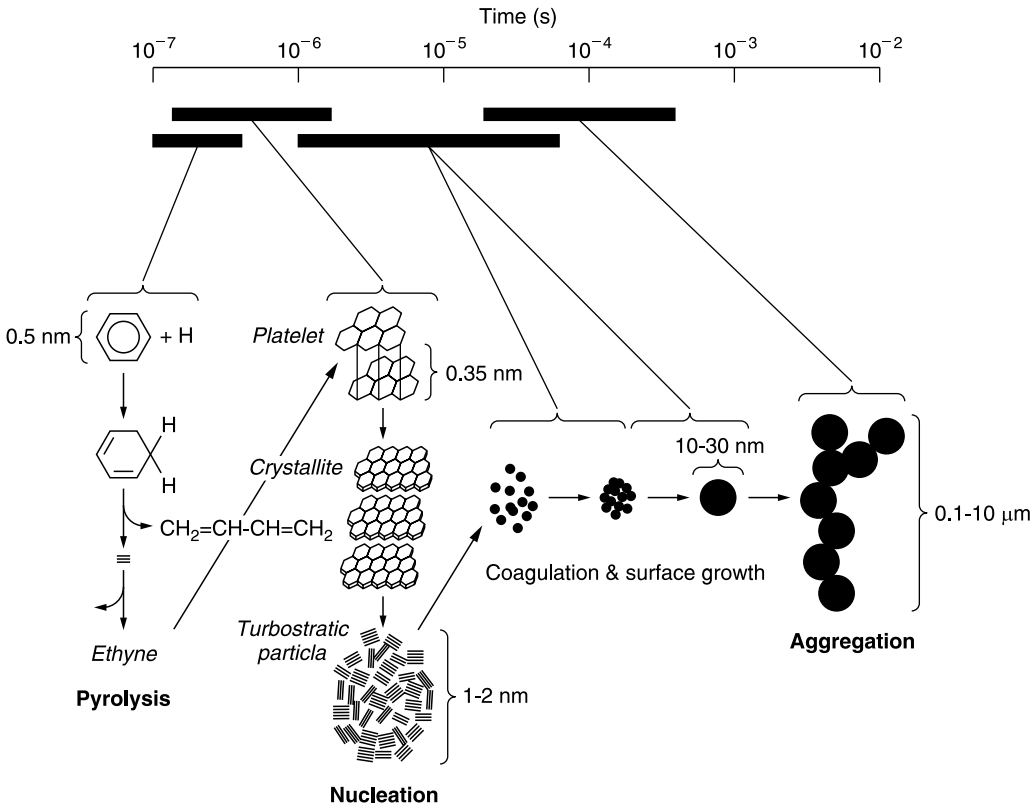


**FIGURE 19.3** Formation of soot particle; a schematic mechanism [7].

**TABLE 19.1**
**Typical Conditions of Diesel Exhaust [9–13]**

| | CO (vppm) | HC (vppm) | $SO_2$ (vppm) | $NO_x$ (vppm) | PM ($g/m^3$) | Exhaust temp. (°C) | Exhaust flow rate ($m^3/h$) |
|---|---|---|---|---|---|---|---|
| Passenger car | 150–1500 | 20–400 | 10–150 | 50–1400 | 0.01–0.1 | 100–360 | 40–50 |
| Heavy-duty truck | n.q. | n.q. | n.q. | 50–1600 | 0.05–0.25 | 100–450 | 15–125 |

n.q. = not quoted.

found in new clean diesel engines, while the higher numbers are characteristic of older engines [9–13].

### 19.1.2 Environmental and Health Effects of Diesel Particulate Emissions

Particulate matter from diesel engines emitted directly to the air is one of the origins of air pollution. Together with biomass combustion, fuel combustion contributes to the excess of soot particles at the lower troposphere level [14]. In urban areas, where exposure to diesel exhaust may be especially high, diesel engines will be a major source of particulates [15].

**TABLE 19.2**
**U.S. Diesel Engine Emission Standards (g/kWh): Past, Present, and Future**

| Year | THC | CO | $NO_x$ | PM (trucks) | PM (urban buses) |
|---|---|---|---|---|---|
| 1974–1978 | 21.5 | 53.6 | | | |
| 1979–1984 | 2.0 | 33.5 | 13.4[a] | | |
| 1985[b]–1987 | 1.8 | 20.8 | 10.7 | | |
| 1988–1989 | 1.8 | 20.8 | 10.7 | 0.8 | 0.8 |
| 1990 | 1.8 | 20.8 | 8.1 | 0.8 | 0.8 |
| 1991–1992 | 1.8 | 20.8 | 6.7 | 0.3 | 0.3 |
| 1993 | 1.8 | 20.8 | 6.7 | 0.34 | 0.13 |
| 1994–1995 | 1.8 | 20.8 | 6.7 | 0.13 | 0.09 |
| 1996–1997 | 1.8 | 20.8 | 6.7 | 0.13 | 0.07 |
| 1998–2003 | 1.8 | 20.8 | 5.4 | 0.13 | 0.07 |
| 2004 | — | 20.8 | 3.4[a] | 0.13 | 0.07 |
| 2007 | — | 20.8 | 1.48[a] | 0.014 | 0.014 |
| 2010 | — | 20.8 | 0.27[a] | 0.014 | 0.014 |

[a]$THC + NO_x$ (THC = total hydrocarbon).
[b]Test cycle changed from steady-state to transient operation.

The presence of soot as air pollutant has serious consequences for human health. In general, particles inhaled by humans are segregated by size during deposition within the respiratory system. Larger particles deposit in the upper respiratory tract while smaller inhalable particulates travel deeper into the lungs and are retained for longer periods of time. If the smaller particles are present in greater numbers, they have a greater total surface area than larger particles of the same mass. Therefore, the toxic material carried by small particles is more likely to interact with cells in the lungs than that carried by larger particles [16,17].

Diesel PM smaller than 10 μm, PM10, not only penetrates deeper and remains longer in the lungs than larger particles, but it also contains large quantities of organic materials that may have significant long-term health effects. Linear- and branched-chain hydrocarbons with 14 to 35 carbon atoms, polynuclear aromatic hydrocarbons (PAH), alkylated benzenes, nitro-PAHs, and a variety of polar, oxygenated PAH derivatives are common particulate-bound compounds. Several of them have the potential to be carcinogenic and mutagenic [18,19].

Diesel emission legislation applied in the past forced car manufacturers to comply and reflected levels of diesel emissions with time. In Table 19.2 the U.S. emissions regulations for heavy-duty trucks and urban buses are presented as an example.

### 19.1.3 Strategies in Diesel Engine Emissions Control

The emissions of diesel engines are greatly influenced by engine variables such as combustion chamber design, air/fuel ratio, rate of air/fuel mixing, and fuel injection timing and pressure. For a diesel engine the emissions of PM and $NO_x$ have an inverse correlation. An effort to reduce soot particles is always associated with an increase in $NO_x$. This is called the trade-off of soot and $NO_x$. For example, so-called exhaust gas recirculation (EGR) and retarded injection can reduce the $NO_x$ emission, but at the same time increase particulate emission (Figure 19.4, curve 1). However, high-pressure injection and cooled EGR can suppress the particulate emission but they increase $NO_x$ emissions (Figure 19.4, curve 2)

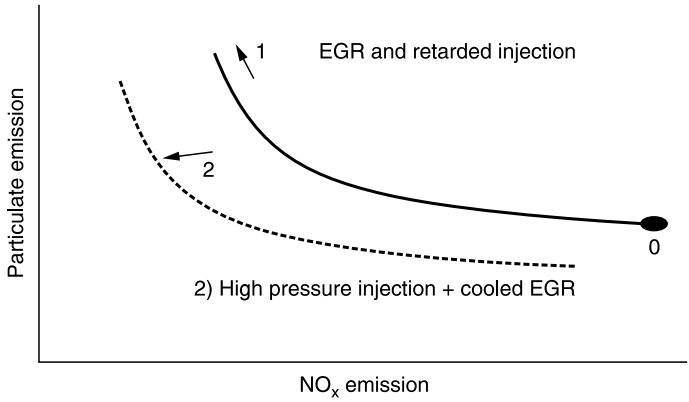


**FIGURE 19.4** Trade-off of diesel particulate and $NO_x$ emissions. (After Neeft, J.P.A., Makkee, M., and Moulijn, J.A., *Fuel Process. Technol.*, 47, 1–69, 1996.)

In general, diesel engine emissions can be minimized via engine modifications, fuel reformulation, and exhaust after-treatment systems. The major effort of the automotive industry in transition of the compressed ignition process into a homogeneous ignition process is not described here since it is beyond the scope of this chapter. The homogeneous ignition process will prevent nonuniform behavior in the combustion process and will lead to substantially lower $NO_x$ and soot emissions. This homogeneous ignition process will be the main research and development effort of the automotive industry, since it can perhaps prevent the need for after-treatment devices to clean the exhaust gas. In this chapter only the role of catalysis for comprehensive control of diesel engine emissions via after-treatment technology is outlined. A detailed discussion in this chapter will focus on the catalysis of dry soot particulate oxidation as an important element in diesel particulate emissions control.

Two methods are commonly employed for reducing the PM from diesel engines: diesel oxidation catalysts (DOCs) and diesel particulate filters (DPFs) or traps. The catalyst supports used in these applications are completely different. The DOC oxidizes CO, HC, and the soluble organic fraction (SOF), while the DPF traps particulates through a wall-flow filter, ceramic fiber filter, or ceramic foam. With advances in engine design, low-sulfur fuel, sensor technology, and ceramic compositions, the DOCs and DPFs will become standard equipment for control of particulate emissions from passenger cars, buses, and trucks.

## 19.2 DIESEL OXIDATION CATALYST FOR SOF, CO, AND HC OXIDATION

Recent advances in diesel technology have lowered the amount of exhaust particulates significantly such that DOCs have provided the required incremental particle removal for MY $1994^+$ vehicles. The DOCs use flow-through cordierite substrates with large frontal area (see Figure 19.5) [21]. Depending on the type of engine and its exhaust, they oxidize 30 to 80% of the gaseous HC and 40 to 90% of the CO present. They do not alter $NO_x$ emissions. DOCs have been used in more than 60,000 diesel fork lift trucks and mining vehicles since 1967 for reducing HC and CO emissions [22].

DOCs have little effect on dry soot (carbon), but engine tests show that they typically remove 30 to 50% of total particulate load. This is achieved by oxidizing 50 to 80% of the SOFs present. DOCs are less effective with "dry" engines in which particulates have a very low SOF content [22].

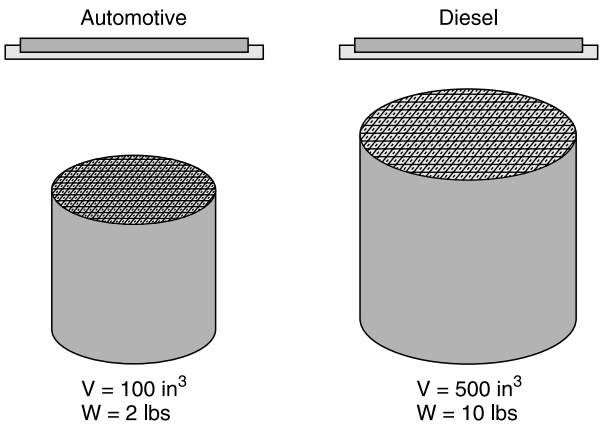


**FIGURE 19.5** Relative size of automotive versus diesel substrates (After Gulati, S.T., SAE Paper, 920145, 1992.).

DOCs are very different from those used for gasoline; however, they do use a monolithic honeycomb support. Gases flow through the honeycomb with minimum pressure drop and react with the catalyst on the walls of the channels.

Although both metal and ceramic supports have been used, ceramic substrates offer stronger catalyst adhesion, less sensitivity to corrosion, and lower cost. The use of ceramics in automotive converters gives additional confidence in their performance.

Catalytic sites promote the reaction between HC gases, including those that would condense as SOFs downstream, and oxygen to form carbon dioxide and water. These sites also oxidize liquid SOFs, whether they are droplets that contact the catalyst or SOF gases that adsorb on them. SOFs adsorbed or condensed on the porous carrier are volatilized and then oxidized at the catalytic sites.

DOCs have to function in a demanding environment. Although diesel exhaust temperatures are well below those in gasoline engine exhaust (373 to 723 K vs. 573 to 1373 K), diesel catalysts must contend with solids, liquids, and gases (not just gases), and deposits of noncombustible additives from lubricating oil. The latter contain zinc, phosphorus, antimony, calcium, magnesium, and other contaminants that can shorten catalyst life below that mandated. Contamination also can come from sulfur dioxide in the exhaust.

Catalyst life might be extended by the development of low-ash lubricating oils and by modifying carrier properties such as surface chemistry, pore structure, and surface area to create contamination-resistant catalysts. Another avenue is periodic regeneration to remove contaminants.

The physical durability of DOCs depends heavily on mechanical and thermal properties of catalyzed substrates and their operating conditions (see Table 19.3).

Since diesel exhaust is substantially colder than that from a gasoline engine, and since the conversion temperature for diesel emissions is considerably lower, the thermal stresses associated with radial and axial temperature gradients in catalytic converters are well below the threshold strength thereby eliminating thermal fatigue potential and ensuring crack-free operation over the required 500,000 km. With thermal durability under control, the mechanical durability takes on a major focus to ensure total durability. To this end, it is necessary to ascertain high mechanical strength of the coated monolith, build in a resilient packaging system, and ensure positive and moderately high mounting pressure to guard against vibrational and impact loads. Much like automotive catalysts, the DOCs can continue to function catalytically even in a fractured state as long as there is sufficient

**TABLE 19.3**
**Operating Conditions for Automotive versus Diesel Catalysts**

| | Automotive | Diesel |
|---|---|---|
| Temperature range (°C) | 300–1100 | 100–550 |
| Temperature gradient (°C) | 100–300 | 100–200 |
| RH (%) | $<100$ | 100 |
| Space velocity (l/l/h) | 30,000–100,000 | 60,000–150,000 |
| Vibration acceleration ($g$) | 28 | 10–20 |

From Gulati, S., in *Structured Catalysts and Reactors*, Cybulski, A. and Moulijn, J.A., Eds., Marcel Dekker, New York, 1996, pp. 15–58 and 501–542. Courtesy of Marcel Dekker, New York.

mounting pressure to keep the cracks shut and adequate catalytic activity to oxidize organic particulates over the required 500,000 km, i.e., the packaging design is just as important as catalyst formulation to meet the 500,000 km durability.

The circular contour of DOCs is ideal from the packaging point of view because it experiences a uniform mounting pressure and an axisymmetric temperature distribution both of which are beneficial to long-term durability. However, since the DOC is both larger and heavier and may experience different vibrational loads than the automotive catalyst, its mounting design requires special considerations. Moreover, since its operating temperature is lower than the intumescent temperature of ceramic mats, the converter assembly must be preheated to remove the organic binder and ensure adequate mounting pressure before installation [23].

Finally, since packaging plays a key role in preserving the mechanical integrity of a diesel converter, both the mat thickness and its mounting density must be carefully tailored to provide substantial mounting pressure on the monolith to meet the 500,000 km durability. Guided by the successful packaging designs for European automotive converters and North American heavy-duty gasoline truck converters, both subjected to harsher driving conditions, a 6200 g/m$^2$ mat with a mount density of 1 g/cm$^3$ would be a good starting point. Such a design would result in a nominal mounting pressure of 3 bar which is 10 times the minimum required value. It would also enhance the initial tangential strength of DOCs and help contain any partial fragments over the required 500,000 km should the converter experience any cracking.

## 19.3 CATALYSIS FOR OXIDATION OF DRY DIESEL SOOT

In the early 1980s great advances were made with diesel particle trapping techniques. The wall-flow monolith was developed and it was found that particulate emissions could be controlled without having to make engine adjustments. It was thought that a method for oxidizing the trapped soot fraction of diesel PM would be discovered quickly. A catalytic device like the three-way catalyst for gasoline engines was seen as unreliable, since the onset temperature of around 800 K of the soot combustion catalysts of those days was too high for spontaneous regeneration [24]. The general regeneration strategy for noncatalytic oxidation has been to load substantially the trap with soot, ignite the soot by raising the temperature in the presence of available oxygen in the exhaust gas, and then switch the heating off. The required high temperature for completion of regeneration is maintained by the energy released during the exothermic soot combustion reaction. The mechanism is known as self-supporting flame propagation [25]. This type of regeneration can easily get out of control and

damage the filter due to chaotic thermal runaways. The regeneration is influenced by many variables like temperature, oxygen concentration, deposited soot amounts, and mass-gas flow rate. These conditions should remain within certain limits to guarantee safe regeneration. This is in conflict with the demand that a trap should be able to regenerate during all driving conditions without the intervention of the driver. Another problem was inadequate regeneration efficiency: Up to 35% of the soot can remain on the filter. This is undesirable because it will create a soot gradient buildup, which can lead, when finally ignited, to extremely high temperature gradients within the filter.

In the last two decades a number of materials have been explored as catalysts for diesel soot oxidation. The fact that in diesel exhaust $O_2$ is available excessively (4 to 10%) has influenced the development of catalysts for the oxidation of soot. The exploration for the catalyst was initially focused on the direct contact between catalyst and soot in order to decrease the C–$O_2$ reaction temperature, which is generally, as mentioned before, above 800 K for the noncatalytic soot oxidation. Furthermore, the catalytic oxidation of soot is slow, since the solid soot particles are large and, when deposited, immobile. They cannot penetrate into the catalyst's micro- or mesopores where catalytic processes usually take place. Soot oxidation takes place mainly on the filter walls of the particle filter where the catalyst has been deposited.

### 19.3.1 Direct Contact Diesel Soot Oxidation Catalysts

The development of a direct contact soot oxidation catalyst is problematic, since it is difficult to realize a direct contact with the solid soot under real exhaust conditions. Inui and Otowa [26] and Löwe and Mendoza-Frohn [27] were among the first to realize that the contact of deposited soot on a catalytic filter is poor. Neeft et al. [28,29] systematically investigated the effect that the degree of physical contact has on catalytic soot combustion. They mixed soot and catalyst powders with a spatula and defined that as loose contact; they did the same with a mechanical mill and defined that as tight contact; they filtered diesel soot from an exhaust stream on a bed of catalyst particles and defined that as *in situ* contact. Combustion temperature differences as large as 200 K were found between loose and tight contact samples of one catalyst. It is clear that Neeft et al. measured apparent activities that were a function of intrinsic activity and the degree of physical interaction. They found that with the *in situ* samples, the combustion temperatures were similar to the combustion temperatures of loose contact samples and concluded that the contact that arises during practical conditions is similar to loose contact, as illustrated in Figure 19.6.

There are various reasons as to why tight contact mixtures are more reactive: (1) the catalyst will have more contact points with the soot; (2) the catalyst particles will be smaller and better dispersed; and (3) Mul et al. [30] found that the type of contact controls the actual mechanism. They found that for $V_2O_5$ and $MoO_3$ a redox and spill-over mechanism occurs simultaneously in tight contact, whereas in loose contact only the spill-over mechanism will occur. They expected that for soot oxidation in a catalytic filter, oxygen spill-over would be the predominant mechanism.

Watabe et al. [31] were the first to report a catalyst based on a formulation of Cu/K/M/(Cl), where M is V, Mo, or Nb. For years, catalysts based on this formulation were extensively investigated [28,29,32–42] because they exhibited high soot oxidation rates at low temperatures. The high activity was related to the mobility and volatility of the active copper oxychloride component of the catalyst [43]. Unfortunately, catalyst compounds evaporated during soot oxidation [32,39] and, therefore, the catalyst had to be kept below 625 K at all times [39], which made the feasibility of the catalyst questionable [32]. This mobility probably explains why the stability of some of those reported catalysts was low. Querini et al. [44]

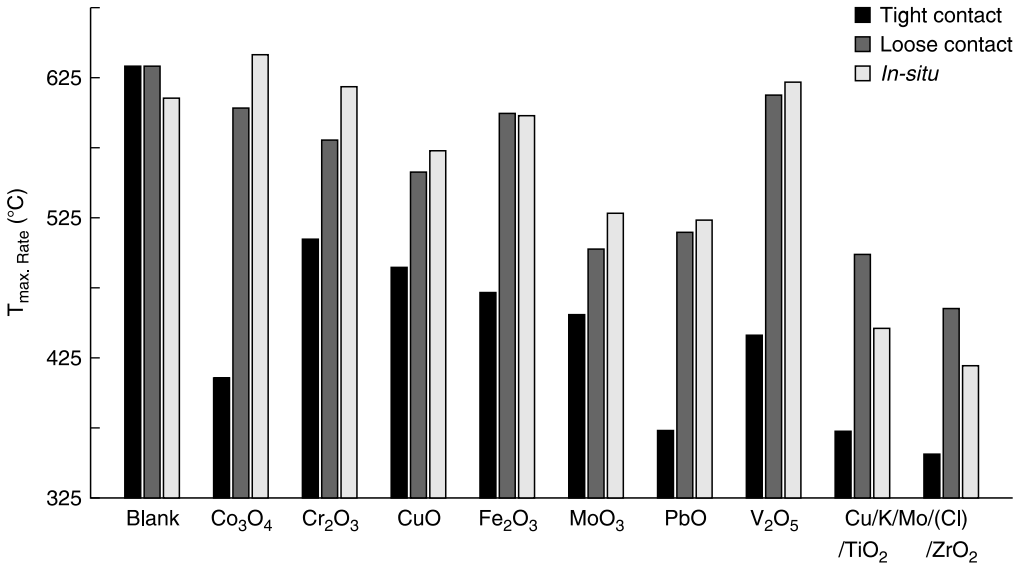


**FIGURE 19.6** Comparison between combustion temperatures of soot collected on catalyst powder (*in situ*) and tight and loose contact combustion temperature. (After Neeft, J.P.A., van Pruisen, O.P., Makkee, M., and Moulijn, J.A., *Appl. Catal. B*, 12, 21–31, 1997.)

stated that the high activity of Co/MgO and Co/K/MgO could be caused by enhanced catalyst mobility afforded by potassium. Badini et al. [40,45] reported that KCl:$KVO_3$ and KI:$KVO_3$ are active catalysts, but they also reported the emission of volatile components of the catalyst. Ahlström and Odenbrand [46] and Moulijn and co-workers [47–52] reported mobile catalysts that did not evaporate during soot oxidation. This type of liquid contact occurs in both laboratory test and pilot plant scale. These types of mobile materials, like $Cs_2SO_4$–$V_2O_5$ (melting point of 647 K), $CsVO_3$–$MoO_3$ (melting point of 650 K), and KCl–$KVO_3$ (melting point of 760 K), demonstrate high activity for oxidation of soot [47–50]. This is primarily due to the *in situ* tight contact between soot and catalyst in its molten state. However, the stability of this type of liquid catalyst might be too low under severe exhaust conditions. Figure 19.7 shows the different types of contact, namely solid catalyst, mobile catalyst, and liquid catalyst.

A good way of improving the quality of induced self-supporting regeneration of a particle filter is to increase the reactivity of soot with a built-in metal catalyst. Such a catalyst can be incorporated during the soot formation process. Blending a stable organometallic additive into the fuel (typically 10 to 100 ppm) is the most convenient method. These catalytic fuel additives are also known as fuel-borne catalysts and result in quasi-continuous regeneration [51].

Catalytic fuel additives were investigated for passive regeneration. During passive regeneration, a trap regenerates itself without the intervention of on-board diagnostic and control systems. Passive regeneration is often a continuous process and, therefore, is referred to as continuous regeneration. During continuous passive regeneration, catalytic fuel additives bring the rate of soot oxidation in equilibrium with the rate of soot deposition, which causes a constant pressure drop over the filter defined as the balance temperature. Lepperhoff et al. [51] compared cerium, iron, and copper additives. They found the lowest balance temperatures for iron and copper to be 625 K. Jelles et al. [52] measured balance temperatures for different mixed additives to discover whether synergetic effects could play a role. They found that after some time of running on low-concentration fuel additive

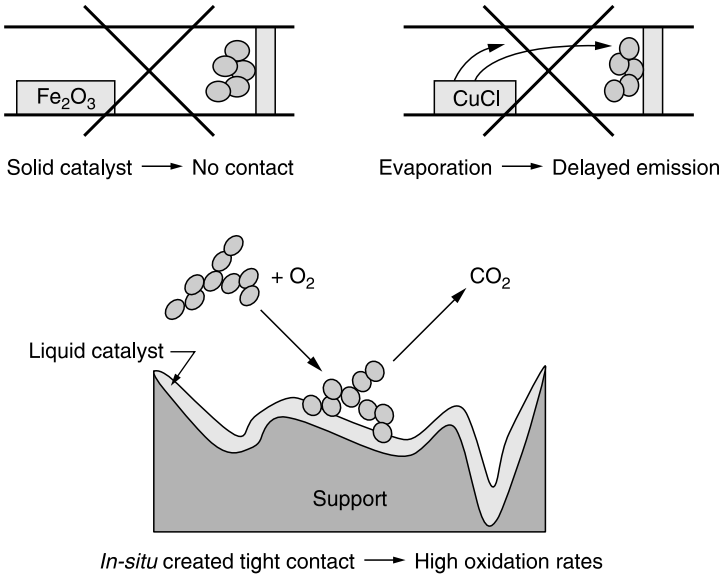


**FIGURE 19.7** Types of catalyst–soot contact: the solid catalyst, the mobile catalyst, and the liquid catalyst.

combinations, there was a dramatic reduction in balance temperature. The reduced balance temperature was explained as follows. Platinum, which was deposited on the monolith, catalyzes the oxidation of NO to $NO_2$. $NO_2$ subsequently reacts with the fuel additive-catalyzed soot. The enhanced activity is explained by assuming that each $NO_x$ molecule is used many times, as illustrated in Figure 19.8.

Figure 19.9 shows a reaction scheme of the proposed mechanism of oxidation of soot by using platinum/cerium fuel additive. Road trials of the mixed catalysts showed that not only the regeneration of filter was altered but so was fuel combustion. The fuel efficiency increased by 5 to 7% and, at the same time, a decrease of particulate mass of 10 to 25% was observed.

Figure 19.10 shows the influence of various after-treatment configurations for fuel additives on balance temperature. The balance temperature is the lowest temperature where soot mass conversion rate is in equilibrium with the soot deposition rate [52,53]. If the wall-flow monolith is partially replaced with platinum-catalyzed ceramic foam, the lowest balance temperature of 550 K for a diesel fuel containing up to 500 ppm sulfur is observed [52]. It should be noted that the reported balance temperature strongly depends on several factors

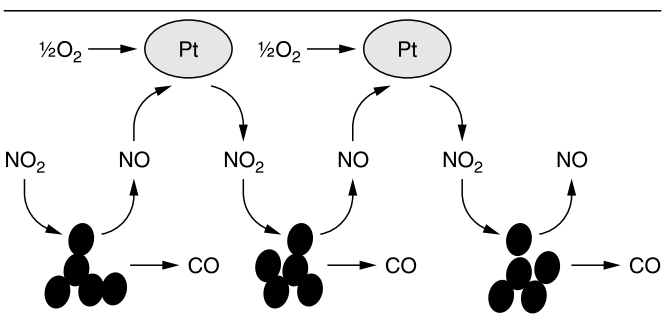


**FIGURE 19.8** Multicycle reaction of NO to $NO_2$ by platinum catalyst following soot oxidation by $NO_2$.

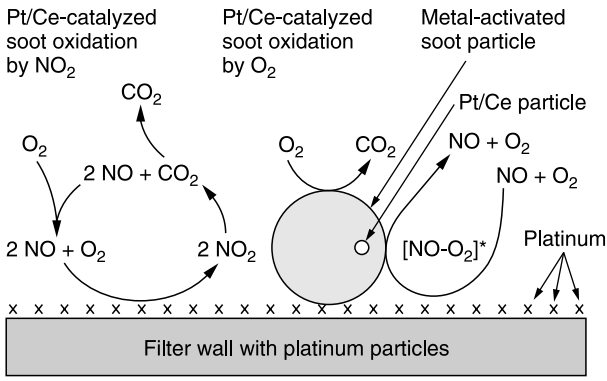


**FIGURE 19.9** Proposed oxidation mechanism for the platinum/cerium fuel additive in combination with a platinum-catalyzed particulate trap. NO is oxidized to $NO_2$ over supported platinum. Subsequently, the formed $NO_2$ oxidizes the soot, forming NO. In parallel, a platinum/cerium-catalyzed oxidation with $O_2$ occurs.

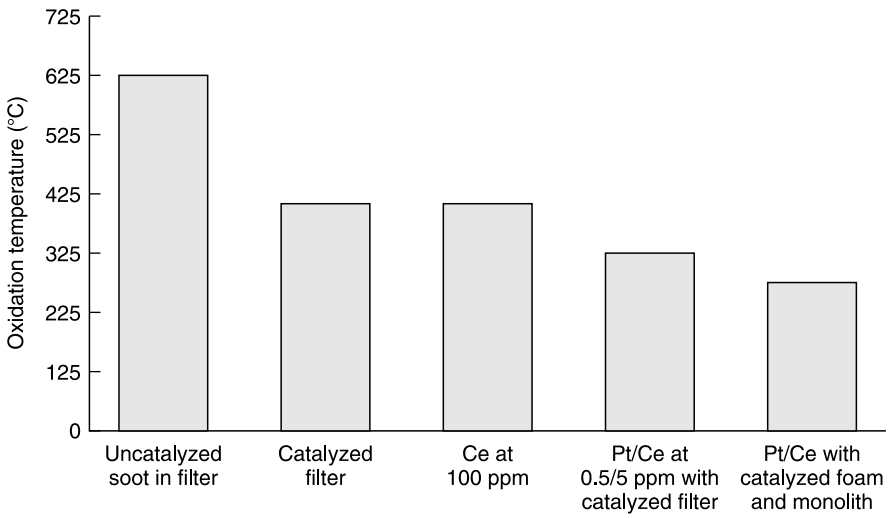


**FIGURE 19.10** Comparison of the oxidation temperature of cerium and platinum/cerium-catalyzed diesel soot. (After Jelles, S.J., Krul, R., Makkee, M., and Moulijn, J.A., *Catal. Today*, 53, 623–630, 1999 and Valentine, J.M., Peter-Hoblyn, J.D., and Acress, G.K., SAE 2000 Spring Fuel and Lubricants Meeting and Exposition, Paris, June 2000, 2000-01-1934.)

such as PM loading, trap volume, trap materials, trap pore size, additive concentration, oxygen concentration, engine type, and engine load.

### 19.3.2 Indirect Contact Catalysts for Diesel Soot Oxidation

Some catalysts can oxidize soot without having intimate physical contact. They catalyze the formation of a mobile compound ($NO_2$, $O_{ads}$, etc.) that is more reactive than $O_2$. In the absence of physical contact, the formation of those mobile species is the main advantageous property of this type of catalyst. For indirect contact catalysts, two main reaction mechanisms are known: $NO_x$-aided gas-phase mechanism and spill-over mechanism.

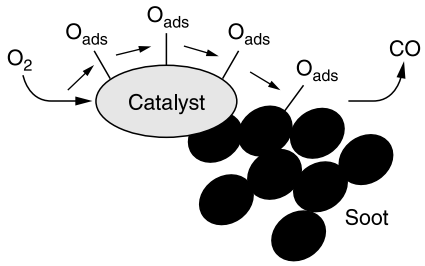


**FIGURE 19.11** Spill-over mechanism in metal oxide-catalyzed soot oxidation.

Cooper and Thoss [54] patented a way of using gas-phase $NO_2$ as an activated mobile species for soot oxidation ($NO_x$-aided gas-phase mechanism) in combination with a filter device. The reaction of $NO_2$ with carbon material was published as early as 1956 [55]. They proposed that $NO_2$ accelerates soot combustion:

$$NO + 1/2\,O_2 \underset{}{\overset{Pt}{\rightleftharpoons}} NO_2 \tag{19.1}$$

$$NO_2 + C \rightarrow CO + NO \tag{19.2}$$

$$NO_2 + CO \rightarrow CO_2 + NO \tag{19.3}$$

Some catalysts can dissociate oxygen and transfer it to the soot particle, where it reacts as if it were in a noncatalytic reaction. This mechanism is known as the spill-over mechanism (Figure 19.11).

There are some examples that show that contact is not a prerequisite in this type of reaction. For instance, Baumgarten and Schuck [56] showed that the rate of catalytic coke oxidation can be accelerated while there is no direct contact between the catalyst and the coke, which they explained by oxygen spill-over. Baker and Chludzinksi [57] showed that $Cr_2O_3$ could accelerate edge recession of graphite while being motionless. Mul et al. [30] showed with a labeled oxygen study that spill-over and redox oxidation can occur simultaneously. They discussed that the dominating mechanism will depend on the degree of physical contact between the catalyst and soot.

## 19.4 DESIGN/SIZING OF DIESEL PARTICULATE FILTER

The filter concept shown in Figure 19.12 involves having the alternate cell openings on one end of the unit plugged in checkerboard fashion. The opposite end or face is plugged

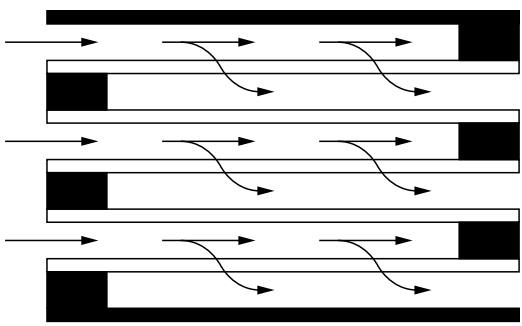

**FIGURE 19.12** Wall-flow filter concept with alternate plugged cells.

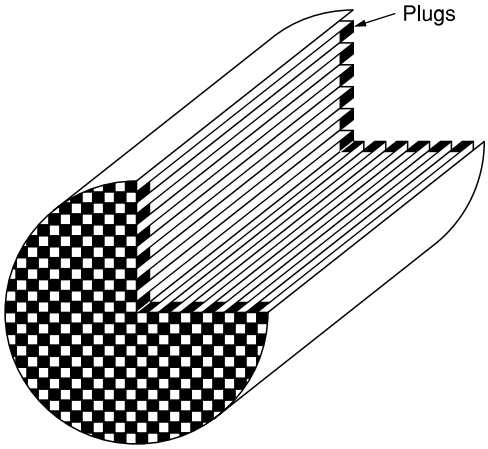


**FIGURE 19.13** Schematic of diesel filter with checkerboard plug pattern.

in a similar manner, but one cell displaced, allowing no direct path through the unit from one end to the other as indicated in Figure 19.13. The exhaust gas entering the upstream end is therefore forced through the porous wall separating the channels and exits through the opposite end by way of an adjacent channel. In this way, the walls of the honeycomb are the filter medium [58,59].

They can be made sufficiently porous to allow exhaust gas to pass through without excessive pressure drop. This wall-flow concept offers a large amount of filter surface area in a reasonably compact volume together with high filtration efficiency. Periodically, the soot that is collected is oxidized to $CO_2$ — a process known as regeneration — which renders the filter clean. The fact that the filter is constructed of special ceramic materials results in its ability to withstanding high temperatures while being chemically inert. One of these materials is a porous cordierite ceramic with magnesia/alumina/silica composition ($2MgO{\cdot}2Al_2O_3{\cdot}5SiO_2$). A key property of this composition is a very low coefficient of thermal expansion. The material used to plug the cell openings in the faces is similar in nature to the body in composition and thermal characteristics. It is a high temperature foaming cement which during firing seals to the cell walls and is impervious to gas flow. More advanced materials capable of withstanding even higher temperature are discussed later. The walls contain a series of interconnected pores of a volume and size sufficient to enable the exhaust gas to flow completely through but restrain most of the particles.

The performance characteristics of wall-flow filter can be varied and managed. Its collection efficiency can be controlled to a large degree by the properties of the walls that form the channels. These include total pore volume, pore size distribution, and the thickness of the wall itself. The flow through the wall can be made more restrictive by adjusting the porosity of the wall. A smaller pore volume creates a highly efficient filter but at the same time restricts the flow and produces high back pressure. Conversely, with porosity adjusted in the opposite direction, low back pressure is achieved, but at the expense of reduction in collection efficiency.

### 19.4.1 Performance Requirements

The four basic requirements that the DPF should meet are [60]:

1. Adequate filtration efficiency to satisfy particulate emissions legislation.
2. Low pressure drop to minimize fuel penalty and conserve engine power.

3. High thermal shock resistance to ensure filter integrity during regeneration.
4. High surface area per unit volume for compact packaging.

Although a high filtration efficiency would make the filter more effective, it must not be accomplished at the expense of high back pressure or low thermal integrity. Indeed, the microstructure and plugging pattern of a ceramic filter can be tailored to obtain filtration efficiencies ranging from 50 to 95% per engine manufacturers' specification. Furthermore, recent advances in ceramic composition have led to filters with high filtration efficiency, acceptable back pressure, and excellent thermal integrity [61–65]. As the PM is trapped in the filter walls, it begins to build up on the surface of open cells forming a soot layer which also acts as a filter. With increasing thickness of soot layer the hydraulic diameter of the channel decreases resulting in higher back pressure. Obviously, the initial and final channel size must be controlled via filter design and soot accumulation level to limit the back pressure to an acceptable value. Again, this can be accomplished by designing the microstructure, the cell geometry, the plugging pattern, and the size of ceramic filter, which in turn are dictated by engine size, flow rate, and engine-out emissions.

The dominant component of trapped particulates is soot carbon which is formed during combustion of a fuel-rich mixture in the absence of adequate oxygen. Although some of the soot may be oxidized to $CO_2$ during the latter part of power stroke, a major portion does not get oxidized due to slow process [66]. The other major component of PM consists of heavy unburned hydrocarbons. Since the chemical energy of soot carbon and heavy hydrocarbons is high, once they are ignited during regeneration they release a great deal of heat which, if not dissipated continuously, can result in high temperature gradients within the filter [67]. Thermal stresses associated with such gradients must be kept below the fatigue threshold value of the filter material to ensure thermal integrity over its lifetime [67,68]. This is best accomplished by using a ceramic composition with ultralow thermal expansion and modestly high fatigue threshold value [61]. Other approaches to improving thermal integrity include the use of fuel additives and/or catalysts to effect regeneration at lower temperatures [69]. Alternatively, more frequent regenerations can also reduce the temperature gradients and enhance thermal integrity but at the expense of fuel penalty if a burner is used for regeneration.

The honeycomb configuration of ceramic filters offers high surface area per unit volume, thereby permitting a compact filter size [70]. The absolute filtration surface area depends on cell size, filter volume, and plugging pattern, all of which are design parameters whose optimization, as will be shown shortly, calls for trade-offs in pressure drop, filtration efficiency, mechanical durability, thermal integrity, and space availability.

### 19.4.2 Composition and Microstructure

The filter composition that has performed successfully over the past two decades is cordierite ceramic with the chemical formula of $2MgO{\cdot}2Al_2O_3{\cdot}5SiO_2$. Its unique advantages include low thermal expansion, ideal for thermal shock resistance, and tailorable microstructure to meet filtration and pressure drop requirements. The extrusion technology for producing automotive catalyst supports also helps manufacture diesel filters. Consequently, the unit cell design can be achieved via die design while the porosity and microstructure are best controlled by composition and process modifications.

The most common cell density employed for diesel filters is 100 cells/in$^2$ with 0.017 in (0.043 cm) thick cell wall. This choice offers the best compromise in terms of filtration area and back pressure. While 200 cells/in$^2$ structure offers 41% larger filtration area and has been used for diesel filters, it results in higher pressure drop. Similarly, thicker cell walls (0.025 in or 0.064 cm thick) offer 50% higher strength but they too result in higher pressure drop.

Another parameter that affects pressure drop is mean pore size, which can range from 12 to 35 μm. Although the pressure drop decreases with increasing pore size, so does filtration efficiency. Hence, a compromise is necessary in tailoring the pore size, wall thickness, and cell density. The wall porosity also affects pressure drop and mechanical strength. Both pressure drop and mechanical strength decrease as the wall porosity increases, thus calling for a compromise in selecting the wall porosity. Most filter compositions and manufacturing processes are designed to yield a wall porosity of 45 to 50%. Filters with low mean pore size are designed to offer high filtration efficiency (>90%), those with intermediate mean pore size are designed for medium filtration efficiency (80 to 90%), and those with large mean pore size are designed for low filtration efficiency (60 to 75%).

### 19.4.3 Cell Configuration and Plugging Pattern

Figure 19.13 shows the wall-flow filter with square cell configuration and checkerboard plugging pattern. The open frontal area (OFA) and specific filtration area (SFA) for such a filter are defined in terms of cell spacing $L$ and wall thickness $t$:

$$\text{OFA} = 0.5\left(\frac{L-t}{L}\right)^2 \tag{19.4}$$

$$\text{SFA} = \frac{2(L-t)}{L^2} \tag{19.5}$$

Since the cell density $N$ for square cell structure is given by

$$N = \frac{1}{L^2} \tag{19.6}$$

it follows from Equation (19.5) that the specific filtration area is directly proportional to the cell density. As the cell density increases, the hydraulic diameter defined by

$$D_h = L - t \tag{19.7}$$

decreases. Hence a portion of the total pressure drop due to gas flow through the open channels of the filter, which depends inversely on the square of hydraulic diameter, increases. Thus, care must be exercised in selecting the appropriate cell density [70]. Other factors that play a key role in designing the filter are its mechanical integrity and filtration capacity. The former is defined by the mechanical integrity factor MIF, which, for a given wall porosity, depends on cell geometry via

$$\text{MIF} = \frac{t^2}{L(L-t)} \tag{19.8}$$

The filtration capacity is the total amount of soot that can be collected prior to safe regeneration. It is directly related to total filtration area TFA defined by the product of specific filtration area and filter volume:

$$\text{TFA} = \frac{2(L-t)}{L^2} V_f \tag{19.9}$$

where the filter volume $V_f$ is given by

$$V_f = \frac{\pi}{4} d^2 l \tag{19.10}$$

in which $d$ and $l$ denote filter diameter and length, respectively.

As noted earlier, most filter compositions enjoy 50% wall porosity to limit the pressure drop to acceptable levels. The mean pore size, which also has a bearing on pressure drop due to gas flow through the wall, is primarily dictated by filtration efficiency requirement. As emissions legislation becomes more stringent, filtration efficiencies $\geq$90% become desirable calling for mean pore diameter of 12 to 14 μm. With microstructure fixed in this manner, the two common cell configurations for diesel filters that have been manufactured are 100/17 and 200/12. It may be verified that they have identical open frontal area and mechanical integrity factor. However, the specific filtration area of 200/12 is 41.5% greater than that of 100/17 configurations implying lower (for constant total filtration area) filter volume for the former, which may be desirable to meet space constraints. However, the hydraulic diameter of 200/12 is 30% smaller than that of 100/17 configurations implying higher pressure drop for the former, which may not be acceptable. Furthermore, the 200/12 configurations may also experience fouling due to ash buildup following several regenerations. The model for total pressure drop is discussed in a later section; however, for a comparison of two different cell configurations we need to write the expression for pressure drop, under fully developed laminar flow conditions, due to gas flow through open channels, $\triangle p_{ch}$, namely

$$\Delta p_{ch} = \frac{C v_{ch} l}{D_h^2} \tag{19.11}$$

where $C$ is a constant and $v_{ch}$ denotes gas velocity through the channel, which is given by

$$v_{ch} = \frac{Q}{A_{open}} \tag{19.12}$$

Here $Q$ is the flow rate through the filter and $A_{open}$ is the open cross-sectional area given by

$$A_{open} = \frac{\pi}{4} d^2 \times \text{OFA} \tag{19.13}$$

In view of identical open frontal area, filters with 100/17 and 200/12 cell configurations will have identical open cross-sectional area and gas velocity through their respective channels under constant flow rate conditions. Thus, the pressure drop $\triangle p_{ch}$ will now be proportional to $l/D_h{}^2$ according to Equation (19.11). We define this ratio as "back pressure index" or BPI:

$$\text{BPI} = \frac{l}{D_h^2} \tag{19.14}$$

Since the specific filtration area of 200/12 configuration is 41.5% greater, the filter length with such a configuration can be 58.5% smaller than that of the filter with 100/17 cell configuration for identical total filtration area. In this manner, Equation (19.14) helps estimate the back pressure penalty (the pressure drop due to channel flow is a significant fraction of total pressure drop through the filter) due to smaller hydraulic diameter of 200/12 cell configuration. The results of this exercise are summarized in Table 19.4, which compares the properties and performance parameters of filters with two different cell configurations.

**TABLE 19.4**
**Properties and Performance Parameters of Diesel Filters with Two Different Cell Configurations and Constant Total Filtration Area**

| Property and performance parameter | 100/17 cell | 200/12 cell |
|---|---|---|
| $L$ (cm) | 0.254 | 0.180 |
| $t$ (cm) | 0.043 | 0.030 |
| $N$ (cells/in$^2$) | 100 | 200 |
| OFA | 0.345 | 0.345 |
| MIF | 0.035 | 0.035 |
| $D_h$ (cm) | 0.211 | 0.150 |
| SFA (cm$^2$/cm$^3$) | 6.54 | 9.25 |
| BPI (cm$^{-1}$) | 1.0 | 1.17 |
| TFA (cm$^2$) | X | X |
| $l$ (cm) | 1 | 0.585l |

From Gulati, S., in *Structured Catalysts and Reactors*, Cybulski, A. and Moulijn, J.A., Eds., Marcel Dekker, New York, 1996, pp. 15–58 and 501–542. Courtesy of Marcel Dekker, New York.

It shows that despite the compact volume of the 200/12 filter it will experience 17% higher back pressure than the 100/17 filter. Such a back-pressure penalty, as is shown later, may well exceed 17% as the soot membrane begins to build up on the surfaces of open channel walls. In addition the pressure drop through porous walls can also be significant. It is clear from Table 19.4 that filter design often calls for trade-offs in performance parameters that, in turn, require prioritization of durability and performance requirements on the part of filter designer.

### 19.4.4 Filter Size and Contour

Both mechanical and thermal durability requirements favor a circular contour for the filter since it lends itself to robust packaging and at the same time experiences less severe temperature gradients during regeneration. Furthermore, circular filters are easier to manufacture and control tolerances, making them more cost effective than noncircular contours. Indeed, the latter have also been manufactured for special applications where space constraint is the dominating factor.

Filter size is generally dictated by engine capacity and is normally equal to engine volume. This "rule of thumb" for designing the filter size has worked well in both mobile and stationary applications in that it helps control soot collection and regeneration without impairing filter durability and imposing high back-pressure penalty. We illustrate these benefits with a realistic example.

Consider a 10-liter, 170 kW diesel engine for a medium- to heavy-duty truck for urban areas. We design the total filter volume to be 10 liters with a microstructure commensurate with 90% filtration efficiency. Based on prior experience we limit the soot loading to 10 g/liter of filter volume to ensure safe regeneration at intervals of two hours. Then

$$\text{Total soot collected} = \frac{10 \times 10}{2} = 50\,\text{g/h}$$

$$\text{Rate of soot emitted by engine} = \frac{50}{0.9} = 55.5\,\text{g/h}$$

which in standard units works out to 0.18 g/kWh. This is a good representation of soot output of new modern-day diesel engines. Let us note that the filter will help reduce the soot emissions from 0.18 to 0.018 g/kWh due to its 90% collection efficiency.

In the next section we develop the pressure drop model and estimate the back pressure due to the above loading.

### 19.4.5 Pressure Drop Model

The pressure drop model is based on the following assumptions [72]:

1. Incompressible gas
2. Laminar flow
3. Constant density and viscosity at a given temperature
4. Cylindrical pores in filter walls
5. No cross-flow between pores

Referring to Figure 19.14, the total pressure drop across the filter is made up of five components:

$$\Delta p_{\text{total}} = \Delta p_{\text{en}} + \Delta p_{\text{ch}} + \Delta p_{\text{w}} + \Delta p_{\text{s}} + \Delta p_{\text{ex}} \tag{19.15}$$

The entrance and exit losses, $\triangle p_{\text{en}}$ and $\triangle p_{\text{ex}}$, are relatively small compared with other losses. Hence they will be neglected. The remaining three losses can be estimated from the generic equation for a circular pipe:

$$\Delta p = \frac{32\mu v l}{g d^2} \tag{19.16}$$

where $\mu$ = gas viscosity (kg/m/sec), $v$ = gas velocity through pipe (m/sec), $l$ = effective pipe length (m), $d$ = effective pipe diameter (m), and $g$ = gravitational acceleration (m/sec/sec).

We will apply the above equation to estimate each component of pressure drop through a 10-liter filter (26.67 cm diameter × 17.78 cm long) with 100/17 cell configuration. To this end, we assume engine size = 10 liters, engine speed = 1500 rpm, gas temperature = 325°C. Then

$$Q = \text{flow rate} = 7500\,\text{l/ min at } 325^\circ\text{C}$$

For the checkerboard plug pattern (we assume a diameter of 10 in (25.4 cm) for the checkerboard region due to fully plugged peripheral region, 0.25 in (0.635 cm) wide)

$$A_{\text{open}} = 175\,\text{cm}^2$$
$$v_{\text{ch}} = \frac{Q}{A_{\text{open}}} = 14.4\,\text{mm/s}$$
$$d_{\text{ch}} = (L - t) = 0.207\,\text{cm}$$

Substituting the above quantities in Equation (19.16) gives

$$\Delta p_{\text{ch}} = \frac{32\mu\, v_{\text{ch}}\, l}{g\, d_{\text{ch}}^2} = 5\,\text{mbar} \tag{19.17}$$

The effective length of pores in the filter wall depends on their tortuosity and mean pore diameter, which for the filter will be taken as 12.5 μm. The effective pore length is

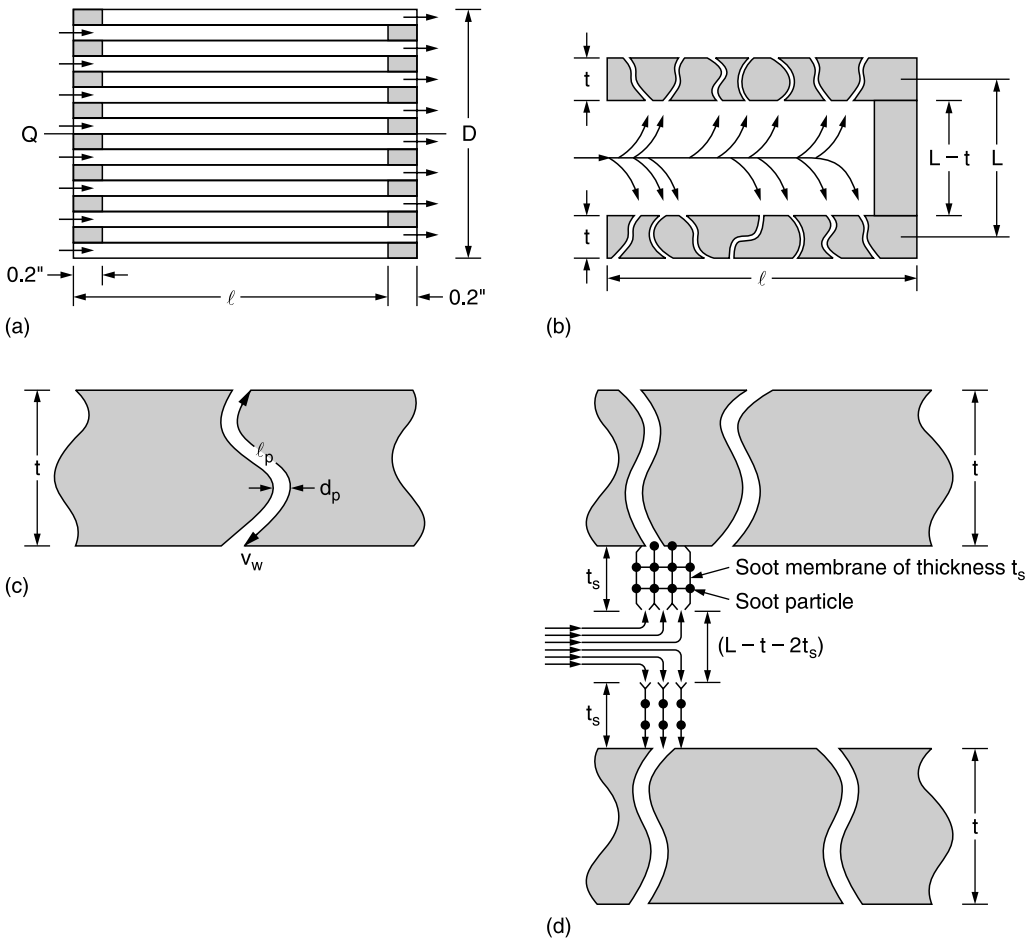


**FIGURE 19.14** Flow model for pressure drop calculations: (a) entry and exit losses; (b) pressure drop through clean channel; (c) pressure drop through cell wall; (d) pressure drop through sooted channel.

approximately $3t$, with $t$ being wall thickness [72]. The gas velocity through the pores is readily obtained by the continuity equation:

$$v_{ch}(L-t)^2 = v_w \times 4P(L-t)l \tag{19.18}$$

where $P$ denotes fractional porosity of filter walls which will be taken as 0.5. Substituting $L = 0.254\,\text{cm}$, $t = 0.043\,\text{cm}$, $P = 0.5$, and $l = 6.6$ in in Equation (19.18), we obtain

$$v_w = 0.0063; \qquad v_{ch} = 8.93\,\text{cm/sec}$$

Substituting $l_p = 3t = 0.128\,\text{cm}$, $d_p = 12.5\,\mu\text{m}$, and $v_w = 8.93\,\text{cm/sec}$ in Equation (19.16) we obtain

$$\Delta p_w = 7\,\text{mbar}$$

Thus, pressure drop through the wall is 38% higher than that through the channel. The above estimate of $\Delta p_w$ is based on clean and open pores. As these pores accumulate

soot, their mean diameter will decrease, the flow velocity will increase and $\Delta p_w$ will go up. To re-estimate $\Delta p_w$, we can still use Equation (19.16) once we know the amount of soot trapped in the pores.

The pressure drop through the soot membrane is negligible due to both its open structure and small thickness. However, as the membrane thickness increases with continuous deposition of soot, the hydraulic diameter of a sooted channel decreases and the gas velocity increases thereby contributing to $\Delta p_{ch}$. To estimate the incremental pressure drop due to soot membrane we must first study the kinetics of soot deposition.

Recall that the maximum allowable soot accumulation for safe regeneration is typically 10 g per liter of filter volume. For a filter volume of 10 liters, the total soot collected prior to regeneration is 100 g over a two-hour filtration cycle. With a filtration efficiency of 90%, the soot output of a 170 kW engine is given by

$$\text{Soot output} = 0.326\,\text{g/kW/h}$$

$$\text{Soot accumulation rate} = \frac{50}{60} = 0.833\,\text{g/min}$$

$$\text{Active filter volume} = 8500\,\text{cm}^3$$

$$\text{Total filteration area} = \text{SFA} \times V_f = 5500\,\text{cm}^2$$

The soot density has been reported in the literature and is approximately 0.056 g/cm$^3$ [60]. Using this value we can estimate the rate at which soot volume, hence the soot membrane thickness, builds up.

$$\text{Rate of soot volume collected per filter} = 14.9\,\text{cm}^3/\text{min}$$

$$\text{Rate of increase in soot membrane thickness} = 0.00028\,\text{cm/min}$$

$$\text{Total thickness of soot membrane after 2 h} = 0.033\,\text{cm}$$

$$d_{ch} = 0.145\,\text{cm}$$

$$A_{open} = 830\,\text{cm}^2$$

$$v_{ch} = \frac{Q}{A_{open}} = 28.9\text{m/sec}$$

Substituting into Equation (19.16), we obtain

$$\Delta p_s = 21\,\text{mbar}$$

Thus, the pressure drop through a sooted channel (with 10 g/l of soot loading) is three times as large as that through the wall and over four times as large as that through the clean channel.

The above computations were also carried out for a 10.5 in diameter × 5 in long filter with 200/12 cell configuration (and identical total filtration area as the 10.5 in diameter × 7 in long filter with 100/17 cell configuration). Table 19.5 compares the individual pressure drop components for the two filters. It is clear from this table that the largest contribution comes from flow through the sooted channel. Furthermore, the small hydraulic diameter of 200/12 cell results in nearly three times higher pressure drop than that for the 100/17 cell which explains the popularity of the 100/17 cell configuration for filter applications.

**TABLE 19.5**
**Comparison of Pressure Drop for Two Filters with Identical Total Filtration Area but Different Cell Configurations (in mbar)**

| | 10.5 in diameter × 7 in length filter (100/17 cell) | 10.5 in diameter × 5 in length filter (200/12 cell) |
|---|---|---|
| $\triangle p_{ch}$ | 5 | 7 |
| $\triangle p_{w}$ | 7 | 10 |
| $\triangle p_{s}$ | 22 | 74 |
| $\triangle p_{total}$ | 34 | 91 |

From Gulati, S., in *Structured Catalysts and Reactors*, Cybulski, A. and Moulijn, J.A., Eds., Marcel Dekker, New York, 1996, pp. 15–58 and 501–542. Courtesy of Marcel Dekker, New York.

The foregoing pressure drop model is only an approximation, which helps quantify the effect of flow rate, open frontal area, and hydraulic diameter. It also provides the relative contributions of open and sooted pores in the wall as well as those of open and sooted channels to the total pressure drop. A more refined model is needed which must correlate well with the experimental data.

## 19.5 PHYSICAL PROPERTIES AND DURABILITY

Physical properties of ceramic diesel filters, which can be controlled independently of geometric properties, have a major impact on their performance and durability. These include microstructure (porosity, pore size distribution, and microcracking), coefficient of thermal expansion (CTE), strength (crush strength, isostatic strength, and modulus of rupture), structural modulus (also called E-modulus), fatigue behavior (represented by dynamic fatigue constant), thermal conductivity, specific heat, and density. These properties depend on both the ceramic composition and the manufacturing process, which can be controlled to yield optimum values for a given application.

The microstructure of diesel filters not only affects physical properties like CTE, strength, and structural modulus, but it also has a strong bearing on filter/catalyst interaction which, in turn, affects the performance and durability of the catalytic filter. The coefficients of thermal expansion, strength, fatigue, and structural modulus of a diesel filter, which also depend on cell orientation and temperature, have a direct impact on its mechanical and thermal durability [73–77]. Finally, since all of the physical properties are affected by washcoat formulation, washcoat loading, and washcoat processing, they must be evaluated before and after the application of the washcoat to assess filter durability.

### 19.5.1 PHYSICAL PROPERTIES

The initial filter compositions were designed to offer a number of microstructures to meet different filtration efficiency and back pressure targets set by engine manufacturers [58]. However, they were not optimized with respect to thermal durability, which became a critical requirement to survive regeneration stresses. A more advanced filter composition, EX-80, with superior performance was developed in 1992. This material is a stable cordierite composition with low CTE and has demonstrated improved long-term durability over a wide range of operating conditions. Moreover, it offers high filtration efficiency and low pressure drop. The low CTE reduces thermal stresses thereby permitting numerous regeneration cycles

**TABLE 19.6**
**Physical Properties of Four Different Diesel Particulate Filters**

| Property | EX-80 (100/17) | EX-80 (200/18) | RC (200/19) | SiC (200/18) |
|---|---|---|---|---|
| **Intrinsic material properties** | | | | |
| Melting point (°C) | ~1470 | ~1470 | ~1470 | ~2400 |
| Density (g/cm$^3$) | 2.51 | 2.51 | 2.51 | 3.24 |
| Specific heat at 500°C (J/g/°C) | 1.11 | 1.11 | 1.11 | 1.12 |
| **DPF material properties** | | | | |
| CTE (22 to 800°C) ($10^{-7}$/°C) | 3.3 | 7.0 | 6.0 | 45.0 |
| Wall porosity (%) | 48 | 50 | 45 | 43 |
| Mean pore size (μm) | 13 | 12 | 13 | 9 |
| Permeability ($10^{-12}$ m$^2$) | 0.61 | 0.61 | 1.12 | 1.24 |
| Axial E-modulus (GPa) | 4.34 | 4.69 | 9.10 | 33.31 |
| Axial MOR (MPa) | 2.83 | 2.83 | 4.67 | 18.62 |
| Thermal conductivity (W/m/°C) | <2 | <2 | <2 | ~20 |
| Thermal shock index (°C) | 1970 | 860 | 855 | 130 |
| Weight density (g/cm$^3$) | 0.46 | 0.46 | 0.70 | 0.85 |
| Heat capacity per unit volume of filter at 500°C (J/cm$^3$/°C) | 0.54 | 0.51 | 0.82 | 0.95 |
| Soot filtration area (1/in) | 16.6 | 23.5 | 21.5 | 21.1 |

From Cutler, W. and Merkel, G., International Fuels and Lubricants Meeting and Exposition, Baltimore, MD, October 2000, SAE 2000-01-2844. Courtesy of SAE.

without impairing the filter's durability. This composition is now one of the industry standards for diesel exhaust after-treatment [61].

Table 19.6 compares the nominal physical properties of EX-80 filter compositions with two different cell structures as well as those of RC 200/17 and SiC 200/18 filters; the latter two are more advanced filters that are discussed in a separate section. The strength and E-modulus data are those measured at room temperature. The axial coefficient of thermal expansion is the average value over the 25 to 800°C temperature range. It is clear from Table 19.6 that the EX-80 filter offers an optimum combination of properties, namely small mean pore size, high strength, low modulus of elasticity (MOE), and low CTE, which together ensure superior performance compared with that of the other filter compositions.

### 19.5.2 Thermal Durability

Thermal durability refers to a filter's ability to withstand both axial and radial temperature gradients during regeneration. These gradients depend on soot distribution, soot loading, $O_2$ availability, and flow rate, and give rise to thermal stresses, which must be kept below the fatigue threshold of filter material to prevent cracking. A detailed analysis of thermal stresses requires the temperature distribution, which is readily measured with the aid of 0.5 mm diameter, Type K chromel–alumel thermocouples during the regeneration cycle [69–71]. To assess the relative thermal durability of different filter candidates we compute the thermal shock parameter using physical properties data and the following equation:

$$\mathrm{TSP} = \frac{(\mathrm{MOR}/\mathrm{MOE})@T_\mathrm{p}}{\alpha_\mathrm{c}(T_\mathrm{c} - 25) - \alpha_\mathrm{p}(T_\mathrm{p} - 25)} \tag{19.19}$$

**TABLE 19.7**
**Axial Thermal Shock Parameter for Cordierite Ceramic and SiC Diesel Particulate Filters (for $T_p = 294°C$)**

| Temp. (°C) | EX-80 (100/17) | EX-80 (200/12) | SiC (200/18) |
|---|---|---|---|
| 600 | 4.2 | 3.9 | 0.6 |
| 700 | 2.4 | 2.2 | 0.4 |
| 800 | 1.5 | 1.4 | 0.3 |
| 900 | 1.1 | 1.0 | 0.25 |
| 1000 | 0.8 | 0.75 | 0.20 |

From Miwa, S., SAE 2001 World Congress, Detroit, MI, March 2001, 2001-01-0192. Courtesy of SAE.

In the above equation $T_c$ and $T_p$ denote the temperature of center and peripheral regions of the filter during regeneration and $\alpha_c$ and $\alpha_p$ denote the corresponding CTE values. In view of the conical inlet pipe near the peripheral region, there is less gas flow in that region and the temperature $T_p$ is typically 400°C. The center temperature, however, is higher depending on soot loading, $O_2$ content, and flow distribution. We will assume $T_c$ to range from 600°C (low soot loading) to 1000°C (high soot loading) and compute TSP values for each of these $T_c$ values while keeping $T_p = 400°C$. The results of this exercise are summarized in Table 19.7.

Let us note that the TSP values for EX-80 filters are 400 to 700% higher than those for SiC filters due, primarily, to their very low CTE values. The higher TSP value signifies improved thermal shock resistance and extended thermal durability. Alternatively, it permits higher regeneration stresses without impairing the filter's durability. It should be pointed out that Equation (19.19) does not account for 10 times higher thermal conductivity of SiC which will result in higher $T_p$ and higher TSP values. Hence both EX-80 and SiC filters will approach comparable thermal shock resistance, notably at higher regeneration temperatures.

The power law fatigue model [78,79] helps estimate the safe allowable regeneration stress for a specified filter life. Denoting the filter's short-term modulus of rupture by $S_2$, the safe allowable stress $S_1$ is given by

$$S_1 = S_2\left(\frac{t_2}{t_1}\right)^{1/n} \tag{19.20}$$

where $t_1$ denotes the specified filter life, $t_2$ denotes equivalent static time for measuring short-term modulus of rupture, and $n$ denotes the dynamic fatigue constant of filter composition. The latter is obtained by measuring MOR as function of stress rate at temperature $T_p$. For a conservative estimate of $S_1$, the lowest value of $n$ should be used in Equation (19.20). The equivalent static time $t_1$ is defined as the actual test duration for measuring MOR divided by $(n+1)$. Since the typical test duration is 30 sec and the lowest value of $n$ is approximately 29 [61], $t_1 \cong 30/30 \cong 1$ sec. Filter life is generally specified in terms of the number of regeneration cycles over the vehicle's lifetime. We will assume a filter life of 250,000 km with a regeneration interval of 450 km and regeneration duration of 10 min. This translates to $t_1 = 6000$ min $= 360{,}000$ sec. Substituting these values in Equation (19.20), we arrive at a safe allowable stress of 1.7 MPa or 60% of MOR value in axial direction. This superiority of the EX-80 filter derives from its higher fatigue constant and MOR value, which, in turn, are related to its optimized microstructure. The effect of filter size, relative to test specimen, may reduce the allowable stress to 30% of MOR value.

### 19.5.3 Mechanical Durability

The mechanical durability of a ceramic filter depends not only on its tensile and compressive strengths but also on its packaging design [70]. In addition to mechanical stresses due to handling and processing, the filter package must be capable of withstanding in-service stresses induced by gas pulsation, chassis vibration, and road shocks. The design of a robust packaging system for catalyst supports discussed in Section 19.2 is equally applicable to the filter. Table 19.6 demonstrates more than adequate strength for tourniquet canning which is recommended for long-term mechanical durability. In addition, preheat treatment of intumescent mat also promotes mechanical durability [80].

## 19.6 ADVANCES IN DIESEL FILTERS

Both the stringent diesel emission legislation in Japan, North America, and Europe (to be introduced in 2007) and the popularity of diesel passenger cars in Europe have led to new advances in diesel filter technology. With new legislation in the offing one of the automotive manufacturers in Europe (PSA) decided to introduce a noncordierite DPF in MY 2001 diesel passenger cars [24,64]. This created a great opportunity for new filter materials [25,62–65], new filter designs [64,81], and improved detection techniques for soot deposits through increased pressure drop [82]. The motivation for developing new materials stemmed from the need for higher thermal conductivity, higher melting temperature, and higher heat capacity than those of cordierite ceramic to facilitate regeneration under uncontrolled conditions [62].

Uncontrolled regeneration is most often described as an unplanned regeneration in which the combustion of a large amount of accumulated soot occurs under conditions in which the exhaust gas has a low flow rate but high oxygen content, resulting in temperatures that far exceed those of controlled regeneration. For example, operation of a diesel engine at high loads and speeds could produce exhaust temperatures that are sufficiently high to initiate combustion in a filter that is heavily loaded with soot. If the engine were to continue running at these conditions throughout combustion, the low oxygen content of the exhaust gas would result in slow burn, while the higher flow rate of the exhaust would serve effectively to transfer heat away from the filter. Thus, only moderately high regeneration temperatures would be achieved. However, if the engine load were to be dramatically reduced soon after combustion was initiated, such as might occur under near idling conditions, then the exhaust flow rate would decrease and the oxygen content of the exhaust gas would increase. The increased oxygen content would accelerate soot combustion, while the lower exhaust flow rate would be less effective in removing heat from the system to cool the filter. Consequently, excessively high temperatures could be achieved within the filter during this uncontrolled regeneration, potentially causing cracking or melting of the filter.

Similarly, the motivation for new designs stemmed from the need for reducing thermal stresses during uncontrolled regeneration by either limiting the peak regeneration temperature to 1000°C via higher heat capacity [81] or by incorporating stress-relief slits in the filter albeit at the risk of impairing mechanical integrity [64]. In this section, we compare new materials like improved cordierite RC and SiC with the standard cordierite. We then discuss new filter designs and how such designs impact their performance including pressure drop.

### 19.6.1 Improved Cordierite "RC 200/19" Filter

Because there is no known compositional modification that can be made from a cordierite-based ceramic to increase its refractoriness without also increasing its CTE and

compromising its thermal shock resistance, survival of a cordierite filter must rely on modifications in filter design that reduce the maximum temperature the filter will experience during uncontrolled regeneration.

The temperature increase experienced by the filter during a regeneration is inversely proportional to the heat capacity of the filter per unit volume for a given exhaust gas flow rate and soot mass burned per unit volume. The volumetric heat capacity of the filter is equal to the product of the bulk density of the filter and the specific heat of the ceramic comprising the filter. Thus, the temperature increase during regeneration can be reduced simply by increasing the mass per unit volume of cordierite filter [81]. An increase in filter mass per unit volume may be achieved by increasing the filter cell density (cells per unit area) or wall thickness, or decreasing the percent porosity of the filter walls. However, changes in cell geometry or porosity will also have an effect on the pressure drop across the filter. An increase in cell density decreases the pressure drop by virtue of higher geometric surface area while an increase in wall thickness increases the pressure drop due to the increased path length through the wall. Increases in wall thickness are generally limited by the permeability of the ceramic comprising the wall. A decrease in porosity may increase the pressure drop unless the effect can be offset by simultaneous modification of the pore size or pore connectivity.

Development of a cordierite ceramic that exhibits a reduced soot-loaded pressure drop for a given filter geometry, cell density, and wall thickness requires modification of the pore microstructure of the ceramic. This may be achieved, for example, by a change in raw materials, forming parameters, or firing conditions (such as furnace atmosphere, heating rates, peak temperature, and hold time at peak temperature). The best candidate resulting from such modifications was designated "RC filter" with a cell structure of 200/19 [25]. Table 19.6 compares its properties with those of EX-80, 100/17, cordierite filter. Figure 19.15 compares the pore microstructure of EX-80, 100/17 and RC 200/19 filters.

It is clear from these data that the RC 200/19 filter offers 25% higher filtration area, 84% higher wall permeability, 52% higher weight density, and 52% higher heat capacity. The latter helps reduce the peak temperature of the RC 200/19 filter during uncontrolled regeneration thereby compensating for its slightly higher CTE value relative to that of the EX-80, 100/17 filter. Furthermore, both the larger filtration area and higher wall permeability of the RC 200/19 filter should result in a more uniform soot distribution and lower temperature gradient thereby preserving or improving its thermal shock resistance as shown later.

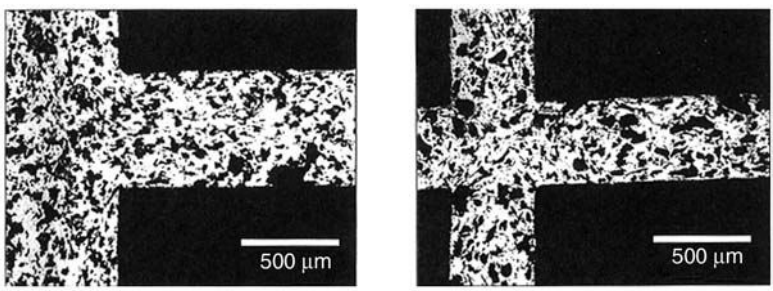


**FIGURE 19.15** Scanning electron micrographs of polished section of (a) RC 200/19 filter wall and (b) EX-80, 100/17 filter wall showing improved pore connectivity of the RC 200/19 filter.

### 19.6.2 SiC Filters

As noted at the beginning of this section, the European automaker PSA introduced a SiC filter in MY 2001 diesel passenger cars due to its high thermal conductivity. Table 19.6 compares the properties of cordierite ceramic, RC 200/19 and SiC 200/18 filters. The latter is a cement-assembled commercial silicon carbide filter from Ibiden. It should be noted that EX-80 cordierite has the lowest intrinsic material density. Moreover, when the specific heat and density of the filter are combined, the heat capacity of the cordierite filter turns out to be lower than that of the SiC filter. A lower heat capacity filter can be heated quickly, resulting in faster regenerations. Faster regeneration generally means lower regeneration fuel penalty if raw fuel injection or additional engine power are required to produce sufficient heat to initiate regular regeneration. While a high heat capacity filter may be desirable for uncontrolled regeneration (to soak up excess heat), a high heat capacity also makes it more difficult to heat the filter for regular controlled regeneration.

Thus, the salient issue comes down to balancing heat capacity of the filter with the material melting point and ash reaction temperature such that the filter regenerates quickly and efficiently during controlled regeneration while still having a sufficiently high melting point and/or ash reaction temperature to prevent pin holes and catastrophic failure during uncontrolled regeneration.

The thermal conductivity of cordierite ($<2$ W/m/K) is much lower than that of SiC ($\sim$20 W/m/K at 500°C). The thermal conductivity for all these materials drops as the temperature increases, such that their conductivity at $\sim$1300°C is half that at 500°C. The value of a high thermal conductivity material is a matter of some debate, as the cooling effect due to high gas flow through the substrate takes heat away from the hot spot much faster than the conductivity can draw the heat away from the hot spot.

The differences in thermal expansion coefficient, E-modulus, and strength among the three materials translate into different thermal shock index (TSI) defined by (MOR/E.CTE). Specifically, the very low CTE and low E-modulus of cordierite materials result in a very high TSI value. This is significant, as cordierite is well known for its excellent thermal shock properties. Despite the high strength of silicon carbide, its high CTE and high elastic modulus lead to a rather low TSI ($<200$). The segmentation of the commercial SiC may represent an effort to limit the distance over which thermal stresses can build.

### 19.6.3 New Filter Designs

As noted earlier, one way to improve a filter's thermal durability is to reduce the peak regeneration temperature by increasing its thermal mass or heat capacity. This is most readily done by modifying the cell design, e.g., by increasing the cell density and wall thickness simultaneously. A series of regeneration tests were conducted on 2 in diameter $\times$ 6 in long (5.08 cm $\times$ 15.24 cm) EX-80 filters, with different cell designs, loaded with 9.6 g/l of soot and the peak regeneration temperature was measured as function of the filter's weight or heat capacity [80]. These data, summarized in Figure 19.16, demonstrate that the peak temperature can be reduced by several hundred degrees by increasing the heat capacity via filter weight. A similar reduction in peak regeneration temperature was observed for the RC 200/19 filter whose heat capacity is 20% higher than that of the EX-80, 100/17 filter (see Figure 19.17) [25].

Another approach to improving thermal durability is to introduce stress-relief slits in the center region of filter, which can reduce thermal stresses by 20 to 70% depending on slit dimensions and location as shown in Figure 19.18 [64]. Of course, these slits must be filled with sealing material to prevent soot-laden exhaust gas from escaping. Regeneration tests on cordierite, SiC, and Si/SiC filters verified that both the improved material properties of the

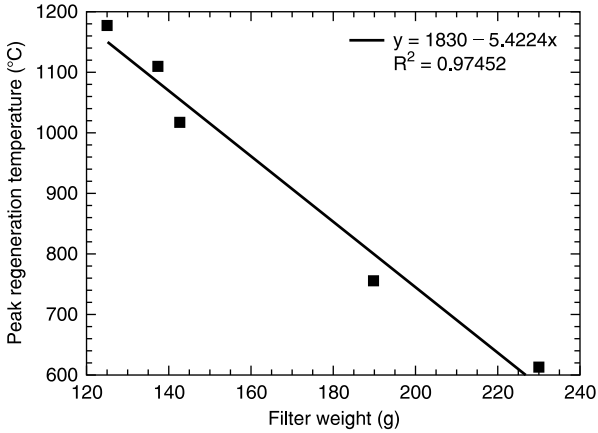


**FIGURE 19.16** Effect of filter weight on peak regeneration temperature.

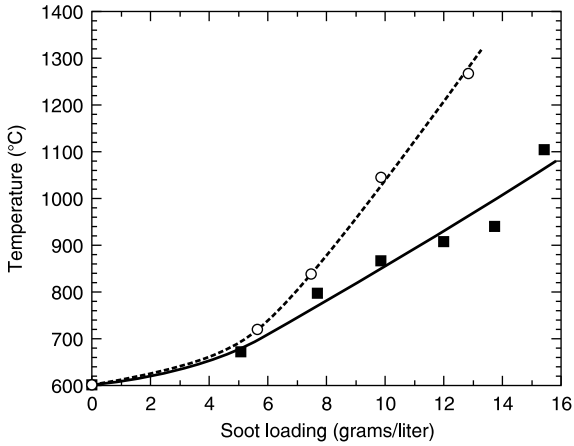


**FIGURE 19.17** Maximum temperature in 14.4 cm × 15 cm filters of RC 200/19 (■) and EX-80, 100/17 (○) during uncontrolled regeneration versus soot loading.

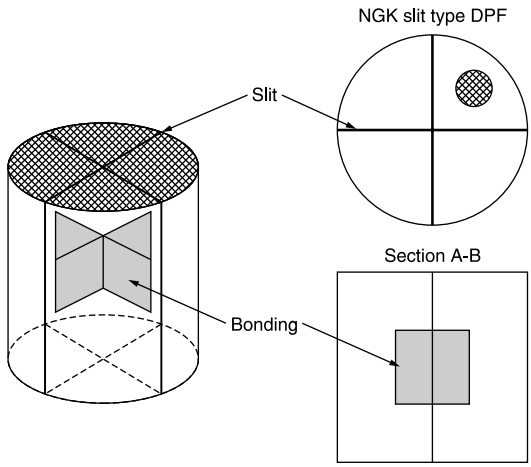


**FIGURE 19.18** Filter design with stress-relief slits.

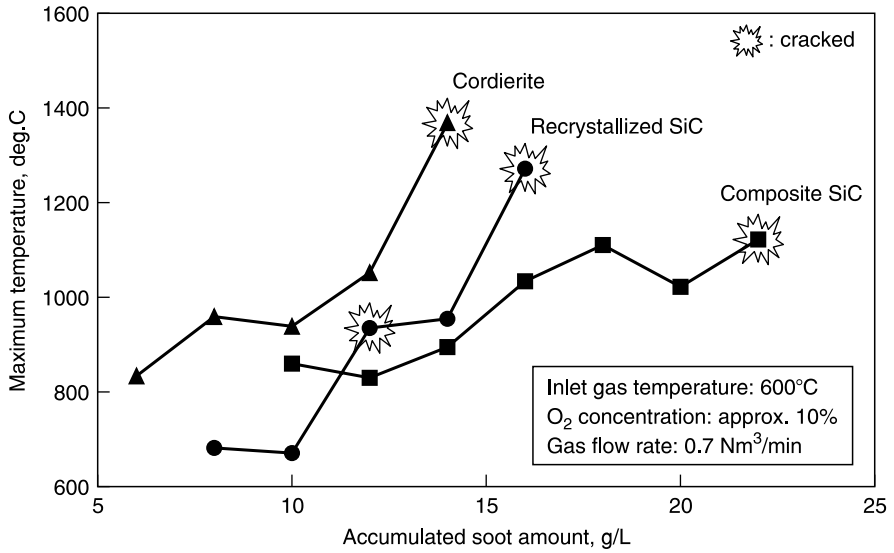


**FIGURE 19.19** Maximum regeneration temperature versus soot loading for three different filters with and without stress-relief slits.

Si/SiC filter and the presence of stress-relief slits helped increase the failure temperature from 900°C (for SiC) to 1100°C with soot loading as high as 22 g/l (see Figure 19.19).

The design approach can also be used to reduce the pressure drop across the filter by increasing its diameter/length ratio while preserving the required filter volume and filtration area [81].

## 19.7 APPLICATIONS

### 19.7.1 Catalytically Induced Regenerated Trap

In the early 2000s PSA Peugeot Citroën introduced a particulate filter system on passenger cars, in which an integrated fuel additive system was applied [83]. This PSA system can be operated with diesel fuel containing up to 500 ppm sulfur. Currently more than 500,000 units are on the market (winter 2003). Their particulate filter system (see Figure 19.20) includes:

1. A filter medium made of silicon carbide with temperature and pressure sensors.
2. An integrated fuel additive system that injects the required quantities of the cerium based catalyst (Eolys$^{TM}$ from Rhodia Terres Rares) whenever the fuel tank is refilled.
3. Common-rail HDI engine monitoring and control software to control filter regeneration and self-diagnosis of the filter.

The pressure sensor monitors filter clogging, and the engine computer initiates the regeneration when necessary. The regeneration involves postcombustion, raising the exhaust fumes to 450°C at the filter inlet. A complete regeneration only requires two to three minutes and is performed every 400 to 500 km without the driver noticing. The cerium-based catalyst additive is dissolved in a solution of 5 g cerium per 100 ml. It is injected into the fuel tank to give the diesel a content of cerium of approximately 25 ppm by weight. The 51 tank of

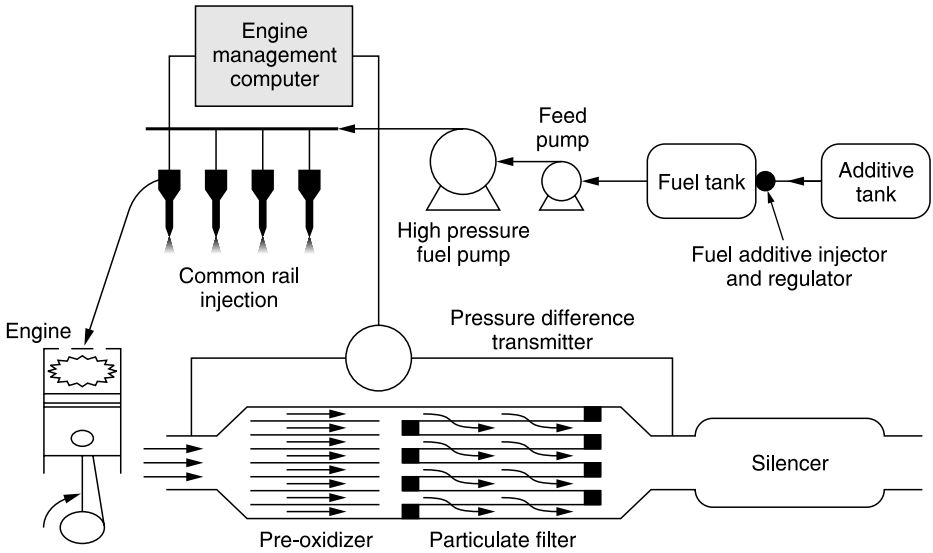


**FIGURE 19.20** Schematic of PSA Peugeot Citroën system.

additive solution ensures a range of 80,000 km. After this 80,000 km the tank can be refilled and the filter cleaned with a water jet to remove the cerium and lubricant ash deposits. For the new type of diesel engine with less soot emission, Rhodia has developed a new type of additive based on cerium and iron [84]. The claimed advantages are that a lower additive dosage rate of only 10 ppm can be used, the regeneration starts at a temperature of around 375°C, and the time needed for regeneration is much shorter. As a result the system is more fuel efficient and the redesigned (larger) filter has only to be cleaned after 300,000 km (probably the lifetime of the engine).

### 19.7.2 Continuously Regenerated Trap

The $NO_x$-aided continuously regenerated trap ($NO_x$-aided CRT) for trucks and buses was developed by Cooper and Thoss [54]. It consists of a wall-flow monolith with an upstream flow-through diesel oxidation catalyst, which is called, in this context, the preoxidizer. Figure 19.21 shows a schematic of the system. The oxidation catalyst converts 90% of the CO and hydrocarbons present to $CO_2$ and $H_2O$, and 20 to 50% of the NO to $NO_2$ [84]. Downstream, the particles are trapped on a cordierite wall-flow monolith and, subsequently, oxidized by $NO_2$.

The modular design of the separated and detachable preoxidizer and filter provide flexibility to the system, which is a great advantage for retrofitting different buses and trucks. In each case, the optimal trap and preoxidizer can be chosen, which in many cases saves space, heat loss, back-pressure, and system costs.

The filter should produce a surplus of $NO_2$ in order to compensate for time intervals in which the temperature is too low for regeneration. The surplus $NO_2$ should not be too high because $NO_2$ is foul smelling in the vicinity of the vehicle, where it has not yet been sufficiently diluted with ambient air. For the environment, compared with NO, $NO_2$ gives no additional problems, because NO converts to $NO_2$ anyway on short timescales [85].

The $NO_x$-aided CRT system, as illustrated in Figure 19.21, is an effective catalytic filter that oxidizes all carbon components in diesel exhaust gas, including small particles and unregulated compounds, while reducing the $NO_x$ concentration by 3 to 8% [86]. It is a simple

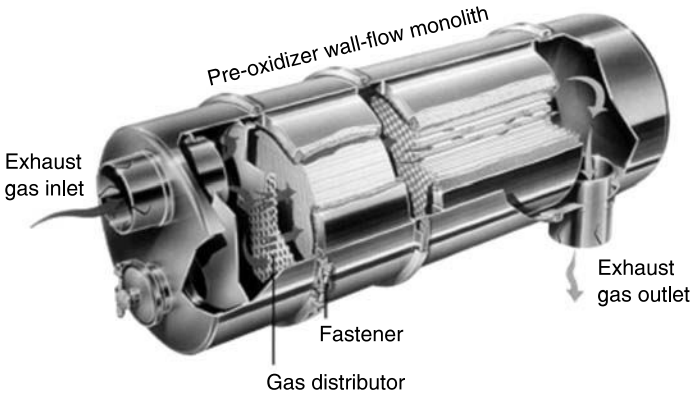


**FIGURE 19.21** Continuously regenerating trap (CRT) system. (Courtesy of Johnson Matthey.)

concept that allows for fit-and-forget usage. The temperature window of 200 to 450°C is reasonable; 200°C is needed for CO and hydrocarbon oxidation [86], whereas 450°C relates to the chemical equilibrium between NO and $NO_2$, which is not favorable above 450°C. The temperature in the filter should be higher than 425°C for at least 40% of the time for effective filter regeneration. The balance temperature is actually higher than 425°C and depends on the fuel sulfur level. The maximum acceptable sulfur level is 30 ppm. Due to continuous regeneration, extreme temperatures are avoided, which enhances filter durability. A satisfactory performance for up to 600,000 km [86] has been reported.

Since the system depends on $NO_x$, it will be uncertain if the required $NO_x$-to-soot ratio for successful regeneration will be met in future engines. One option for less dependency on engine-out $NO_x$ is the multiple usage of available $NO_x$. Therefore, a study to optimize the oxidation of NO to $NO_2$ and the oxidation of soot was carried out. Coating the filter section with platinum to reoxidize NO produced from reactions (19.2) and (19.3) is the latest effort to optimize the system [87].

### 19.7.3 Combined Continuously Regenerated Trap and Catalytically Regenerated Trap

"Active Oxygen" is postulated as a species that plays a role in the newly developed system, the diesel particulate and $NO_x$ reduction (DPNR) Toyota Motors system [88,89]. In the DPNR system a layer of an "active oxygen" storage alkali metal oxide is deposited along diesel soot filtration surface areas. On this layer platinum is dispersed. The "active oxygen" is created by the conversion of gas-phase NO over the platinum into surface nitrate species. These surface nitrates will be decomposed at the interface between the soot and active oxygen layer into very reactive adsorbed oxygen atom and NO. The NO can be reoxidized to surface nitrate and the adsorbed oxygen atom is able to oxidize the deposited soot at 300°C and higher. If the system is not able to convert all deposited soot the back pressure over the filter will increase and trigger the regeneration of trapped soot due to a temperature rise in the filter. This increase in temperature is accomplished by injecting diesel fuel directly in the exhaust stream.

The active oxygen storage material acts at the same time as a $NO_x$ trap. When the $NO_x$ trap has reached its maximal allowable buffer capacity for retaining all $NO_x$ as nitrates, then the $NO_x$ trap needs to be regenerated. CO and HCs can decompose these nitrates into nitrogen. These CO and HCs are generated by running the engine rich or by fuel addition

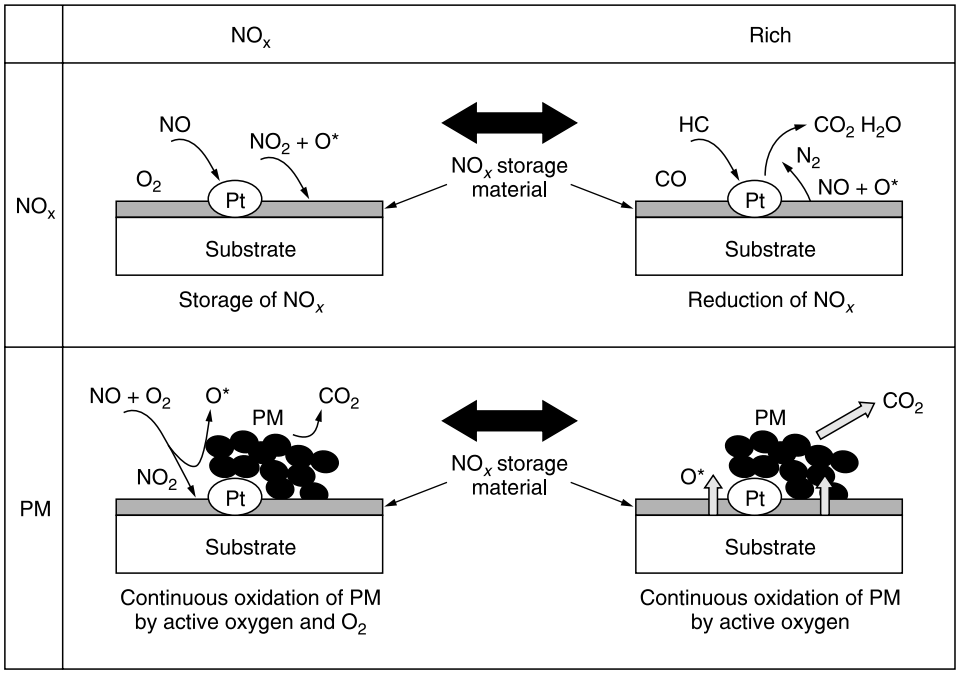


**FIGURE 19.22** Schematic of the diesel particulate and $NO_x$ reduction (DPNR) Toyota Motors system.

into the exhaust stream at a temperature of around 450°C. The newly generated CO and HCs are converted into $CO_2$ by surface nitrates while the nitrates themselves convert mainly to $N_2$ and, to some extent, to NO. In other words, this type of soot oxidation trap acts as a soot abatement technology, while at the same time it acts as a $NO_x$ abatement technology. Figure 19.22 illustrates the chemical processes of the Toyota system.

Total reduction of diesel exhaust emissions (CO, HCs, PM, and $NO_x$) is preferably achieved in a single filter system such as the DPNR system. However, this system may encounter several problems such as engine ash deposit, complexity of data logging, and the effectiveness of engine-out $NO_x$ concentration. It is reported that the fresh DPNR system reduces 80% of $NO_x$ and PM emissions and might meet the U.S. tier 2 bin 5 or 6 emissions standards using low-sulfur diesel fuel [90]. It is evident that a fleet test has to demonstrate the efficiency and robustness of the system.

## 19.8 SUMMARY

The stringent emissions legislation for diesel-powered vehicles has led to new developments in both oxidation catalysts and filters. These developments include new materials for catalyst supports and filters with higher heat capacity, filtration area, and physical durability. In addition, the advent of low-sulfur fuels is helping in developing catalysts to meet the 300,000 km vehicle durability. Similarly, improvements in engine design have reduced particulate matter via more efficient fuel combustion. Furthermore, significant progress is being made in reducing oxides of nitrogen via $NO_x$ adsorbers and DeNOx catalysts. Also, a variety of fuel additives have been developed that help reduce the soot regeneration temperature thereby reducing thermal stresses and enhancing physical durability of diesel filters. Twenty-five years of successful experience with ceramic catalyst supports for

automotive application is proving valuable in designing robust mounting system for diesel oxidation catalysts. In view of considerably lower operating temperature and longer physical durability requirement, relative to automotive catalysts, the intumescent mat used in packaging diesel oxidation catalysts has to be preheated to ensure sufficient holding pressure on the catalyst against inertia, vibration, and road shock loads experienced in service.

Filter materials having a higher melting temperature than cordierite have also been developed and are being used in commercial applications subject to more stringent emissions legislation. These include SiC and RC 200/19, which are able to withstand uncontrolled regeneration due to either their higher conductivity (SiC) or heat capacity (RC 200/19). SiC offers higher thermal conductivity and melting temperature, which are very desirable for uncontrolled soot regeneration, but its order of magnitude higher thermal expansion coefficient can lead to inferior thermal shock resistance [91]. An improved version, namely Si/SiC composite material, has recently been developed which offers low thermal expansion coefficient and superior thermal shock resistance.

Finally, the mounting system can play a major role in ensuring both mechanical and thermal durability of diesel oxidation catalysts and filters notably for heavy-duty trucks with severe operating conditions and 500,000 km vehicle durability requirement. Many of the robust packaging systems employed in automotive applications are equally applicable to both diesel oxidation catalysts and filters.

The successful introduction of the particulate filter system by PSA Peugeot Citroën and the continuous regeneration trap (CRT) by Johnson Matthey are the evidence of persistent and creative research. The catalytic advanced technology of Toyota with their DPNR system is another clear demonstration of high-standard reactor and catalysis engineering.

## NOTATION

| | |
|---|---|
| $A_{open}$ | open cross-sectional area ($m^2$) |
| $c_p$ | specific heat ($J\ kg^{-1}\ K^{-1}$) |
| $C$ | constant in Equation (19.11) |
| $d$ | diameter (m) |
| $D_h$ | hydraulic diameter (m) |
| $g$ | gravitational acceleration ($m\ sec^{-2}$) |
| $k$ | thermal conductivity ($W\ m^{-1}\ K^{-1}$) |
| $l$ | length (m) |
| $L$ | cell spacing (m) |
| $n$ | dynamic fatigue constant |
| $N$ | cell density ($cells\ m^{-2}$) |
| $\Delta p$ | pressure drop (Pa) |
| $P$ | fractional porosity of filter wall |
| $Q$ | flow rate through filter ($m^3\ sec^{-1}$) |
| $S_1$ | safe allowable stress |
| $S_2$ | filter's short-term modulus of rupture |
| $t$ | wall thickness (m) |
| $t_1$ | specified filter life (sec) |
| $t_2$ | equivalent static time (sec) |
| $T$ | temperature (K) |
| $v$ | gas velocity ($m\ sec^{-1}$) |
| $V_f$ | filter volume ($m^3$) |
| $\alpha$ | coefficient of thermal expansion ($K^{-1}$) |
| $\lambda$ | thermal conductivity ($W\ m^{-1}\ K^{-1}$) |

| | |
|---|---|
| $\rho$ | density ($kg\,m_f^{-3}$) |
| $\mu$ | gas viscosity ($kg\,m^{-1}\,sec^{-1}$) |

## Subscripts

| | |
|---|---|
| c | center |
| ch | channel |
| en | entrance |
| ex | exit |
| p | peripheral, pore |
| s | soot |
| w | wall |

## Abbreviations

| | |
|---|---|
| BPI | back-pressure index ($m^{-1}$) |
| CTE | coefficient of thermal expansion ($K^{-1}$) |
| MIF | mechanical integrity factor |
| MOE | modulus of elasticity (Pa) |
| MOR | modulus of rupture (Pa) |
| OFA | open frontal area |
| SFA | specific filtration area ($m^{-1}$) |
| TFA | total filtration area ($m^2$) |
| TSP | thermal shock parameter (K) |

## REFERENCES


1. Yanowitz, J., McCormic, R.L., and Graboski, M.S., In-use emissions from heavy-duty diesel vehicles, *Environ. Sci. Technol.*, 34, 729–740, 2000.
2. Abdel-Rahman, A.A., On the emission from internal-combustion engines: a review, *Int. J. Energy Res.*, 22, 483–513, 1998.
3. Heywood, J.B., *Internal Combustion Engine Fundamentals*, McGraw-Hill, New York, 1988, p. 930.
4. Bérubé, K.A., Jones, T.P., Williamson, B.J., Winters, C., Morgan, A.J., and Richards, R.J., Physicochemical characterisation of diesel exhaust particles: factors for assessing biological activity, *Atmos. Environ.*, 33, 1599–1614, 1999.
5. Mark, J. and Morey, C., *Diesel Passenger Vehicles and the Environment*, Union of Concerned Scientists, Berkeley, CA, 1999, pp. 6–15.
6. Johnson, J.H., Bagley, S.T., Gratz, L.D., and Leddy, D.G., A review of diesel particulate control technology, 1992 Horning memorial award lecture, SAE paper 940233, 1994.
7. Smith, O.I., Fundamentals of soot formation in flames in application to diesel engine particulate emissions, *Prog. Energy Combust. Sci.*, 7, 275–291, 1981.
8. Saitoh, K., Sera, K., Shirai, T., Sato, T., and Odaka, M., Determination of elemental and ionic compositions for diesel exhaust particles by particle induced X-ray emission and ion chromatography analysis, *Anal. Sci.*, 19, 525–528, 2003.
9. Challen, B. and Baranescu, R., Eds., *Diesel Engine Reference Book*, Butterworth-Heinemann, 1999.
10. Lepperhoff, G., Petters, K.-D., Baecker, H., and Pungs, A., The influence of diesel fuel composition on gaseous and particulate emissions, *Int. J. Vehicle Design*, 27, 10–19, 2001.
11. Pattas, K., Samaras, Z., Kyriakis, N., Pistikopoulos, P., Manikas, T., and Seguelong, T., An experimental study of catalytic oxidation of particulates in a diesel filter installed on a direct injection turbo-charged car, *Topics Catal.*, 16/17, 255–262, 2001.

12. Guenther, M., Vaillancourt, M., and Polster, M., Advancements in Exhaust Flow Measurement Technology, SAE 2003 World Congress and Exhibition, Detroit, MI, March 2003, 2003-01-0780.
13. van Setten, B.A.A.L., Makkee, M., and Moulijn, J.A., Science and technology of catalytic diesel particulate filter, *Catal. Rev. Sci. Eng.*, 43, 489–564, 2002.
14. Cooke, W.F. and Wilson, J.J.N., A global black carbon aerosol model, *J. Geophys. Res.*, 101, 19395–19410, 1996.
15. Faiz, A., Weaver, C.S., and Walsh, M.P., *Air Pollution from Motor Vehicles, Standard and Technology for Controlling Emission*, World Bank, Washington, DC, 1996, p. 63.
16. Health Effect Institute, *Understanding the Health Effects of Components of the Particulate Matter Mix: Progress and Next Step*, HEI Perspectives, April 2002, p. 20.
17. Farleigh, A. and Kaplan, L., Danger of Diesel, U.S. Public Interest Research Group Education Fund, 2000, p. 6.
18. Tsien, A., Diaz-Sanxhez, D., Ma, J., and Saxon, A., The organic component of diesel exhaust particles and phenanthrene, a major polyaromatic hydrocarbon constituent, enhances IgE production by IgE-secreting EBV-transformed human B cells in vitro, *Tox. Appl. Pharm.*, 142, 256–263, 1997.
19. http://www.dieselnet.com/standards/intro.html (accessed May 2004).
20. Neeft, J.P.A., Makkee, M., and Moulijn, J.A., Diesel particulate emission control, *Fuel Process. Technol.*, 47, 1–69, 1996.
21. Gulati, S. Design Considerations for Diesel Flow Through Converters, SAE paper 920145, 1992.
22. Farrauto, R., Reducing Truck Diesel Emissions, *Automotive Engineering*, February 1992.
23. Stroom, P., Merry, R.P., and Gulati, S., Systems Approach to Packaging Design for Automotive Catalytic Converters, SAE paper 900500, 1990.
24. Eastwood, P., *Critical Topics in Exhaust Gas Aftertreatment*, Research Studies Press, Baldock, U.K., 2000.
25. Merkel, G., Beall, D., Hickman, D., and Vernacotola, M., Effects of Microstructure and Cell Geometry on Performance of Cordierite Diesel Particulate Filters, SAE 2001 World Congress, Detroit, MI, March 2001, 2001-01-0193.
26. Inui, T., Otawa, T., and Takegami, Y., Enhancement of oxygen transmission in the oxidation of active carbon by composite catalyst, *J. Catal.*, 76, 84–92, 1982.
27. Lôwe, A. and Mendoza-Frohn, C., Zum Problem der Dieselruß-Verbrennung auf einem katalysatorbeschichteten Filter: Der Kontakt zwischen Katalysator und Feststoff, *Chem. Ing. Tech.*, 62, 759–762, 1990.
28. Neeft, J.P.A., Makkee, M., and Moulijn, J.A., Metal oxides as catalysts for the oxidation of soot, *Chem. Eng. J.*, 64, 295–302, 1996.
29. Neeft, J.P.A., van Pruisen, O.P., Makkee, M., and Moulijn, J.A., Catalyst for the oxidation of soot from diesel exhaust gases: II. Contact between soot and catalyst under practical condition, *Appl. Catal. B*, 12, 21–31, 1997.
30. Mul, G., Kapteijn, F., Doornkamp, C., and Moulijn, J.A., Transition metal oxide catalysed carbon black oxidation: a study with $^{18}O_2$, *J. Catal.*, 179, 258–266, 1998.
31. Watabe, Y., Yamada, C., Irako, K., and Murakami, Y., Catalyst for Use in Cleaning Exhaust Gas Particulate, European Patent 0,092,023, October 26, 1983.
32. Mul, G., Neeft, J.P.A., Kapteijn, F., Makkee, M., and Moulijn, J.A., Soot oxidation catalysed by Cu/K/Mo/Cl catalyst: evaluation of the chemistry and performance of the catalyst, *Appl. Catal. B*, 6, 339–352, 1995.
33. Neeft, J.P.A., Schipper, W., Mul, G., Makkee, M., and Moulijn, J.A., Feasibility study towards Cu/K/Mo/(Cl) soot oxidation for the application in diesel exhaust gases, *Appl. Catal. B*, 11, 365–382, 1997.
34. Neeft, J.P.A., Makkee, M., and Moulijn, J.A., Catalyst for the oxidation of soot from diesel exhaust gases: I. An exploratory study, *Appl. Catal. B*, 8, 57–78, 1996.
35. Ciambelli, P., Corbo, P., Parrela, P., Palma, V., and Sciallo, M., Catalytic oxidation from diesel exhaust gases: 1. Screening of metal oxide catalysts by TG-DTG-SDTA analysis, *Thermochim. Acta*, 162, 83–89, 1990.

36. Ciambelli, P., Palma, V., Russo, P., and Vaccaro, S., The effect of NO on Cu/V/K/Cl catalysed soot combustion, *Appl. Catal. B*, 22, L5–L10, 1999.
37. Ciambelli, P., Palma, V., and Vaccaro, S., Low temperature carbon particulate oxidation on a supported Cu/V/K catalyst, *Catal. Today*, 17, 71–78, 1993.
38. Ciambelli, P., Parrella, P., and Vaccaro, S., Kinetic of soot oxidation on potassium–copper–-vanadium catalyst, in *Catalysis and Automotive Pollution Control II*, Vol. 71, Crucq, A., Ed., Elsevier, Amsterdam, 1991, pp. 323–350.
39. Badini, C., Serra, V., Saracco, G., and Montorsi, M., Thermal stability of Cu–K–V catalyst for diesel soot combustion, *Catal. Lett*., 37, 247–254, 1996.
40. Badini, C., Saracco, G., Serra, V., and Specchia, V., Suitability of some promising soot combustion catalyst for application in diesel exhaust after-treatment, *Appl. Catal. B*, 18, 137–150, 1998.
41. Badini, C., Saracco, G., and Serra, V., Combustion of carbonaceous materials by Cu–K–V based catalyst: I. Role of copper and potassium vanadate, *Appl. Catal. B*, 11, 307–328, 1997.
42. Serra, V., Badini, C., Saracco, G., and Specchia, V., Combustion of carbonaceous materials by Cu–K–V based catalyst: II. Reaction mechanism, *Appl. Catal. B*, 11, 329–346, 1997.
43. Mul, G., Kapteijn, F., and Moulijn, J.A., Catalytic oxidation of model soot by metal oxide, *Appl. Catal. B*, 12, 33–47, 1997.
44. Querini, C.A., Ulla, M.A., Requejo, F., Soria, J., Sedrán, U.A., and Miró, E.E., Catalytic combustion of diesel soot particles. Activity and characterisation of Co/MgO and Co, K/MgO catalyst, *Appl. Catal. B*, 15, 5–19, 1998.
45. Badini, C., Saracco, G., and Specchia, V., Combustion of particulate catalysed by mixed potassium vanadates, *Catal. Lett*., 55, 201–206, 1998.
46. Ahlström, A.F. and Odenbrand, C.U.I., Combustion of soot deposit from diesel engines on mixed composite oxide, *Appl. Catal*., 60, 157–172, 1990.
47. Jelles, S.J., van Setten, B.A.A.L., Makkee, M., and Moulijn, J.A., Molten salts as promising catalysts for oxidation of diesel soot: importance of experimental conditions in testing procedures, *Appl. Catal. B*, 21, 35–49, 1999.
48. van Setten, B.A.A.L., Russo, P., Jelles, S.J., Makkee, M., Ciambelli, P., and Moulijn, J.A., Influence of $NO_x$ on soot combustion with supported molten salt catalysts, *React. Kinet. Catal. Lett*., 67, 3–7, 1999.
49. van Setten, B.A.A.L., Jelles, S.J., Makkee, M., and Moulijn, J.A., The potential of supported molten salts in the removal of soot from diesel exhaust gas, *Appl. Catal. B*, 21, 51–61, 1999.
50. van Setten, B.A.A.L., Bremmer, J., Jelles, S.J., Makkee, M., and Moulijn, J.A., Ceramic foam as a potential molten salt oxidation catalyst support in the removal of soot from diesel exhaust gas, *Catal. Today*, 53, 613–621, 1999.
51. Lepperhof, G., Lüders, H., Barthe, P., and Lemaire, J., Quasi-Continuous Particle Trap Regeneration by Cerium Additives, SAE paper 950369, 1995.
52. Jelles, S.J., Krul, R., Makkee, M., and Moulijn, J.A., The influence of $NO_x$ on the oxidation of metal activated soot, *Catal. Today*, 53, 623–630, 1999.
53. Valentine, J.M., Peter-Hoblyn, J.D., and Acress, G.K., Emissions Reduction and Improved Fuel Economy Performance from a Bimetallic Platinum/Cerium Diesel Fuel Additive at Ultra-Low Dose Rate, SAE 2000 Spring Fuel and Lubricants Meeting and Exposition, Paris, June 2000, 2000-01-1934.
54. Cooper, B.J. and Thoss, J.E., Role of NO in Diesel Emission Control, SAE paper 890404, 1989.
55. Arthur, J.R., Ferguson, H.F., and Lauber, K., Comparative rates of the slow combustion of coke in oxygen and nitrogen dioxide, *Nature*, 178, 206–207, 1956.
56. Baumgarten, E. and Schuck, A., Oxygen spillover and possible role in coke burning, *Appl. Catal*., 37, 247–257, 1988.
57. Baker, R.Y.K. and Chludzinski, J.J., Catalytic gasification of graphite by chromium and copper in oxygen, steam, and hydrogen, *Carbon*, 19, 75–82, 1981.
58. Howitt, J. and Montierth, M., Cellular Ceramic Diesel Particulate Filter, SAE paper 810114, 1981.

59. Howitt, J., Elliott, W., Morgan, J., and Dainty, E., Application of a Ceramic Wall-Flow Filter to Underground Diesel Emissions Reduction, SAE paper 830181, 1983.
60. Wade, W., White, J., and Florek, J., Diesel Particulate Trap Regeneration Techniques, SAE paper 810118, 1981.
61. Murtagh, M.J., Sherwood, D., and Socha, L., Development of a Diesel Particulate Composition and Its Effect on Thermal Durability and Filtration Performance, SAE paper 940235, 1994.
62. Cutler, W. and Merkel, G., A New High Temperature Ceramic Material for Diesel Particulate Filter Applications, International Fuels and Lubricants Meeting and Exposition, Baltimore, MD, October 2000, SAE 2000-01-2844.
63. Merkel, G., Cutler, W., and Warren, C., Thermal Durability of Wall-Flow Diesel Particulate Filters, SAE 2001 World Congress, Detroit, MI, March 2001, 2001-01-0190.
64. Miwa, S., Diesel Particulate Filters Made from Newly Developed SiC and Newly Developed Oxide Composite Material, SAE 2001 World Congress, Detroit, MI, March 2001, 2001-01-0192.
65. Ohno, K., Shimato, K., Taoka, N., Santae, H., Ninomiya, T., Komori, T., and Salvat, O., Characterization of SiC-DPF for Passenger Car, SAE 2000 World Congress, Detroit, MI, March 2000, 2000-01-0185.
66. Amann,, C., Stivender, D., Plee, S., and MacDonald, J., Some Rudiments of Diesel Particulate Emissions, SAE paper 800251, 1980.
67. Weaver, C., Particulate Control Technology and Particulate Standards for Heavy Duty Diesel Engines, SAE paper 840174, 1984.
68. Gulati, S. and Helfinstine, J., High Temperature Fatigue in Ceramic Wall-Flow Diesel Filters, SAE paper 850010, 1985.
69. Gulati, S. and Sherwood, D., Dynamic Fatigue Data for Cordierite Ceramic Wall-Flow Diesel Filters, SAE paper 910135, 1991.
70. Gulati, S., Ceramic catalyst supports for gasoline fuel, in *Structured Catalysts and Reactors*, Cybulski, A. and Moulijn, J.A., Eds., Marcel Dekker, New York, 1996, pp. 15–58. Gulati, S., Ceramic catalyst supports and filters for diesel exhaust aftertreatment, in *Structured Catalysts and Reactors*, Cybulski, A. and Moulijn, J.A., Eds., Marcel Dekker, New York, 1996, pp. 501–542.
71. Brown, G., *Unit Operations*, Wiley, New York, 1955.
72. Carman, P., *Flow of Gases through Porous Media*, Butterworth, London, 1956.
73. Gulati, S., Thermal Stresses in Ceramic Wall-Flow Diesel Filters, SAE paper 830079, 1983.
74. Vergeer, H., Gulati, S., Morgan, J., and Dainty, E., Electrical Regeneration of Ceramic Wall-Flow Diesel Filter for Underground Mining Application, SAE paper 850152, 1985.
75. Gulati, S., Strength and Thermal Shock Resistance of Segmented Wall-Flow Diesel Filters, SAE paper 860008, 1986.
76. Gulati, S. and Lambert, D., Fatigue-Free Performance of Ceramic Wall-Flow Diesel Particulate Filter, ENVICERAM'91, Saarbrucken, 1991.
77. Gulati, S., Lambert, D., Hoffman, M., and Tuteja, A., Thermal Durability of Ceramic Wall-Flow Diesel Filter for Light Duty Vehicles, SAE paper 920143, 1992.
78. Wiederhorn, S.M., Subcritical crack growth in ceramics, in *Fracture Mechanics of Ceramics*, Vol. 2, Bradt, R.C., Hasselman, D.P., and Lange, F.F., Eds., Plenum Press, New York, 1974, pp. 613–646.
79. Ritter, J.E., Engineering design and fatigue failure of brittle materials, in *Fracture Mechanics of Ceramics*, Vol. 4, Bradt, R.C., Hasselman, D.P., and Lange, F.F., Eds., Plenum Press, New York, 1978, pp. 667–686.
80. Gulati, S., Sherwood, D., and Corn, S.H., Robust Packaging System for Diesel/Natural Gas Oxidation Catalysts, SAE paper 960471, 1996.
81. Hickman, D., Diesel Particulate Filter Regeneration: Thermal Management Through Filter Design, International Fuels and Lubricants Meeting and Exposition, Baltimore, MD, October 2000, SAE 2000-01-2847.
82. Johnson, T., Diesel Emission Control Technology in Review, SAE 2001 World Congress, Detroit, MI, March 2001, 2001-01-0184.
83. http://www.psa.fr (accessed May 2004).
84. http://www.dieselnet.com/news/0210rhodia.html (accessed September 2003).

85. Hawker, P., Myers, N., Hürthwohl, G., Voge, H.Th., Bates, B., Magnusson, L., and Bronnenberg, P., Experience with a New Particulate Trap Technology in Europe, International Congress and Exposition, Detroit, MI, February 1997, SAE 970182.
86. Allanson, R., Cooper, B.J., Thoss, J.E., Uusimaki, A., Walker, A.P., and Warren, J.P., European Experience of High Mileage Durability of Continuously Regenerating Diesel Particulate Filter, SAE 2000 World Congress, Detroit, MI, March 2000, 2000-01-0480.
87. Allanson, R., Blakeman, P.G., Cooper, B.J., Hess, H., Silcock, P.J., and Walker, A.P., Optimizing the Low Temperature Performance and Regeneration Efficiency of the Continuously Regenerating Diesel Particulate Filter (Cr-DPF) System, SAE 2002 World Congress and Exhibition, Detroit, MI, March 2002, 2002-01-0428.
88. Nakatani, K., Hirota, S., Takeshima, S., Itoh, K., and Tanaka, T., Simultaneous PM and $NO_x$ Reduction System for Diesel Engines, SAE 2002 World Congress and Exhibition, Detroit, MI, March 2002, 2002-01-0957.
89. Itoh, K., Tanaka, T., Hirota, S., Asanuma, T., Kimura, K., and Nakatani, K., Exhaust Purifying Method and Apparatus of an Internal Combustion Engine, U.S. Patent 6,594,991, July 22, 2003.
90. McDonald, J. and Bunker, B., Testing of the Toyota Avensis DPNR at U.S. EPA-NVFEL, SAE paper 2002-01-2877, 2002.
91. Heck, R.M., Farrauto, R.J., and Gulati, S.T., Catalytic Air Pollution Control: Commercial Technology, 2nd Edn., John Wiley & Sons, New York, 2002.